



University of West Attica
School of Engineering
Department of Biomedical Engineering

**Non-intrusive cardiovascular electrocardiogram
monitoring for objective and proactive
management of chronic diseases**

PAPAKONSTANTINOU MARIA

Registration Number: 19388086

Supervisors

David Efstratios, Assistant Professor

Pablo Pérez Tirador, Assistant professor

Athens 08 / 09 / 2024

The Three-Member Examination Committee

Supervisor

Efstratios David

Associate Professor of
Biomedical Engineering
department, University of
West Attica

**Panteleimon
Asvestas**

Professor of Biomedical
Engineering department,
University of West Attica

Dimitrios Glotsos

Professor of Biomedical
Engineering department,
University of West Attica

Signature

Signature

Signature

DECLARATION BY THE AUTHOR OF THE DIPLOMA THESIS

The signatory Maria Papakonstantinou of Sideris and Androniki, with registration number 19388086, student of the Department of Biomedical Engineering of the University of West Attica, I declare responsibly that:

"I am the author of this Diploma Thesis and any help I had for its preparation is fully recognized and referenced. Also, any sources from which I have used data, ideas, or words, whether exact or paraphrased, are listed in their entirety, with full reference to the authors, the publisher, or the journal, including any sources that may have been used by the internet. I also certify that this work has been written exclusively by me and is a product of intellectual property of both myself and the University of West Attica.

Violation of my above academic responsibility is an essential reason for the revocation of my diploma".

Date: **08/ 09/ 2024**

A handwritten signature in black ink, appearing to be the initials 'MP' followed by a stylized flourish.

Signature

CONTENTS

Abstract.....	6
Acknowledgments.....	7
1. Introduction.....	8
1.1 Electrocardiogram (ECG).....	8
1.2 ECG recording.....	9
2. Theoretical background.....	10
2.1 Anatomy of the heart.....	10
2.2 The Cardiac Action Potential.....	11
2.2.1 Depolarization.....	13
2.2.2 Repolarization.....	13
2.2.3 Resting phase.....	13
2.2.4 The cardiac dipole.....	14
2.3 Einthoven ECG triangle.....	14
2.4 Understanding the Electrocardiogram (ECG).....	16
2.4.1 Principle of operation of ECG sensors.....	16
2.4.2 Instrumentation Amplifier.....	17
2.4.3 Filters.....	18
2.4.4 Protection Circuit.....	18
2.4.5 Interfacial electrochemical reaction.....	19
2.4.6 Electrodes.....	19
2.5 Non-contact ECG.....	20
2.5.1 Technological Developments and Innovations.....	20
3. Material and Methods.....	22
3.1 Material.....	22
3.1.1 Equipment.....	23
3.2 Methods.....	27
3.2.1 The first circuit.....	28
3.2.2 Acquisition using two electrodes with fingers.....	32
3.2.4 Experiment with Bitalino and the set up.....	34
3.2.5 Experiment with the circuit and the set up.....	34
3.2.6 Experiment with the circuit, the set up and insulation.....	35
3.2.7 Experiment with the circuit, the set up , insulation and moisture.....	36
3.2.8 Experiment with Bitalino, set up and moisture.....	37
3.2.9 Experiment with the circuit, the set up, insulation and small electrodes.....	37
3.2.10 The final circuit.....	37

3.2.11	Set up for experiments with volunteers.....	38
3.2.12	30 minutes experiment with the circuit2 and a volunteer	39
3.2.13	Experiment with circuit2, volunteers and moisture.	40
3.2.14	Signal Processing	40
4.	Results	43
4.1	Results for the calibration experiment	43
4.1.1	Acquisition using two electrodes with fingers	43
4.1.2	Results for Bitalino with setup.....	44
4.1.3	Results for circuit with set up	47
4.1.4	Results for circuit with set up and insulation	49
4.1.5	Result for circuit with set up, insulation and moisture.....	52
4.1.6	Bitalino with set up and moisture results	54
4.1.7	Results for circuit with set up, insulation and small electrodes	56
4.1.8	Results for circuit2 with set up, insulation and reference	58
4.2	Results for the experiments with volunteers	60
4.2.1	Results for the 30 minutes experiment.....	60
4.2.2	Results for the volunteers experiment with moisture.....	62
5.	Discussion and Conclusions	65
	References.....	67
	APPENDIX 1.....	70
	APPENDIX 2.....	71

TABLE 3.1	SPECIFICATIONS OF THE CONDUCTIVE ELECTRODES	25
TABLE 3.2	EQUIPMENT.....	26
TABLE 3.3	DESCRIPTION OF EACH IMPLEMENTATION	27
TABLE 3.4	COMPONENTS.....	29
TABLE 3.5	DIELECTRIC CONSTANT OF THE MATERIALS	33
TABLE 4.1	BITALINO WITH SET UP RESULTS-CONDUCTIVE SHEET.....	44
TABLE 4.2	BITALINO WITH SET UP RESULTS-CONDUCTIVE TAPE	44
TABLE 4.3	CIRCUIT WITH SET UP RESULTS- CONDUCTIVE SHEET.....	47
TABLE 4.4	CIRCUIT WITH SET UP RESULTS-CONDUCTIVE TAPE	47
TABLE 4.5	CIRCUIT WITH SET UP AND INSULATION RESULTS- CONDUCTIVE SHEET	49
TABLE 4.6	CIRCUIT WITH SET UP AND INSULATION RESULTS-CONDUCTIVE TAPE	49
TABLE 4.7	CIRCUIT WITH SET UP, INSULATION AND MOISTURE RESULTS-CONDUCTIVE TAPE	52
TABLE 4.8	BITALINO WITH INSULATION AND MOISTURE RESULTS-CONDUCTIVE TAPE	54
TABLE 4.9	CIRCUIT WITH SET UP, INSULATION RESULTS AND SMALL ELECTRODES.....	56
TABLE 4.10	CIRCUIT2 WITH SET UP, INSULATION AND REFERENCE	58
TABLE 4.11	RESULTS FROM MSQI METHOD	63

Abstract

This thesis explores the development and implementation of a non-intrusive cardiovascular electrocardiogram (ECG) monitoring system designed for proactive chronic disease management. Traditional ECG methods, using gel and dry electrodes, require direct skin contact, often causing discomfort and irritation. This project addresses these issues using coupled ECG (cECG) technology to acquire signals through clothing. The research involved creating sensorized furniture with integrated sensors for non-intrusive ECG recording. Initially, a circuit with two electrodes was built to conduct preliminary experiments. Extensive characterization of materials and electrodes was performed to optimize configurations for signal acquisition. Various fabrics and conductive materials were tested for their effectiveness in transmitting ECG signals, and electrodes were assessed for conductivity and flexibility. Experiments evaluated the impact of insulation, moisture, and electrode size on signal quality. Then, a second circuit was constructed, adding a reference electrode to facilitate calibration trials. These trials, involving diverse human volunteers, ensured accurate signal capture and assessed the prototype's performance under different conditions. Results indicated that the cECG system effectively captures signals. Increased pressure improved the clarity of the ECG signals, while moisture played a catalytic role in maintaining signal integrity during experiments. In tests with volunteers, 75% were had visible QRS peaks with moisture, while only the 25% without its addition.

Acknowledgments

The present work of thesis was the result of a study experience at the University of San Pablo CEU in Madrid (Spain), developed from February to September 2024 and partially supported by the Erasmus Plus educational program.

I would like to express my deepest gratitude to Professor Abraham Otero and Professor Pablo Pérez Tirador for their guidance, insightful feedback, and support throughout my thesis journey. Their expertise and encouragement have been essential to my academic development. I am also deeply thankful to Associate Professor Stratos David for his consistent help throughout this journey, particularly during my research in Madrid. His support and collaboration have been greatly appreciated.

I am also profoundly thankful to my friend, Vasiliki Katsara, for her constant support and the numerous discussions that helped me refine my ideas. Without their contributions and encouragement, this thesis would not have been possible.

Lastly, I would like to express my deepest love and gratitude to my parents and my brother for their unwavering support over the past five years. Without them, none of this would have been possible.

1. Introduction

1.1 Electrocardiogram (ECG)

Cardiovascular diseases are the main cause of death worldwide, and the trend is exacerbating as emerging countries adopt lifestyle habits from developed countries. Tools are needed to better diagnose and manage this disease to stop this trend. Non-intrusive monitoring during patients' daily lives could play a fundamental role in building these tools.

Electrocardiogram (ECG) monitoring is an essential tool for managing and diagnosing cardiovascular diseases, providing useful information about cardiac function and rhythm. It is a recording of the electrical activity generated by the heart and gives as a result the QRS complex and P, T, U waves (see Figure 1.1). The P wave occurs when the atrium contracts to fill the ventricles with blood. After, the QRS complex represent the contraction of the ventricles, which ending up completely emptied at the end of the ST segment. The T wave represents the repolarization of the ventricles, signifying the restoration of their electrical balance as they prepare for the next cardiac cycle, and is typically a rounded, waveform. Despite its small size and unclear origin, the U wave, when inverted or prominent, indicates underlying medical conditions [1].

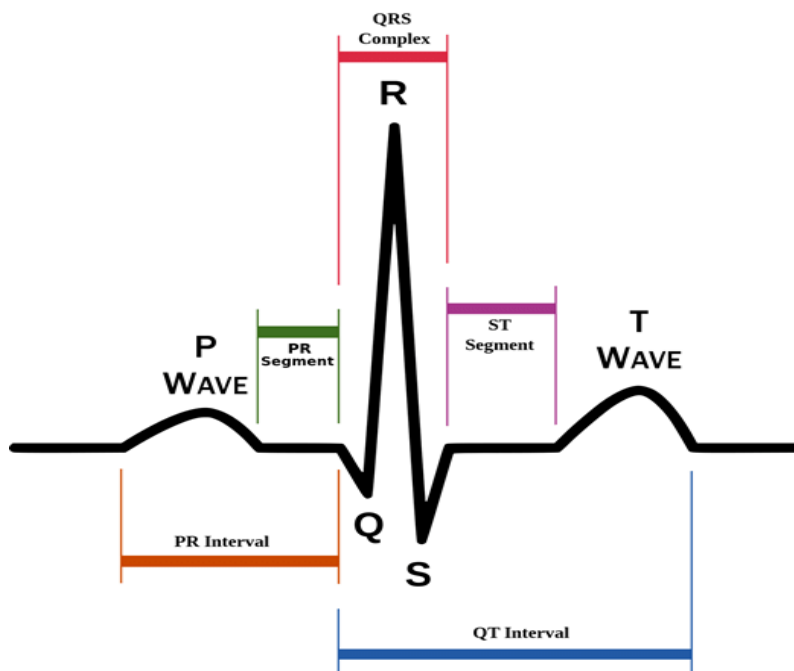


Figure 1.1 Heart waves (PQRST) [1]

1.2 ECG recording

Different types of electrodes, ranging from gel to dry sensors, are employed in the acquisition of ECG signals. The primary problem is that all these electrodes require direct contact with the patient's skin and most of the time, when doctors use gel electrodes, it results in a messy situation due to the gel residue and it can cause irritation because it can be tight or painful. Therefore, it can be concluded that these types of electrodes are uncomfortable and inconvenient for users. Technological solutions are being researched to solve this problem. In recent years, current telemonitoring solutions for ECG recording have been greatly developed. We can find systems like a smart watch, that works simply by touching with a finger while we are still or even through an application on a smart phone. The downside to this is that older people are unfamiliar and face limitations in technology adoption and use.

The second problem is that the recordings have to be taken for a long time in order to detect some cardiac problems. With contact electrodes the patient has two options. The first option is the Holter system, which causes discomfort because it has to be carried around and the cables get in the way. The second option is to go to the clinic, which means that he has to stay in order to have a continuous measurement, and of course that is difficult for the elderly patients. The solution to this problem is remote monitoring of ECG signals which holds immense potential for improving patient care, particularly in the context of chronic diseases and the elderly. In the scientific literature, pilot tests of telemonitoring platforms for the management of chronic diseases with the ability to remotely record ECG can be found. Ergonomics, ease of use, and the perception that the platform is having a positive impact on patient health are key factors in achieving patient acceptance. However, one of the primary reasons for the failure of telemonitoring solutions, particularly in long-term monitoring scenarios like chronic diseases, is the lack of acceptance and adherence [2] [3].

In this study we will use coupled ECG (cECG) to solve the two problems we mentioned above. Unlike dry or wet electrodes, there is no direct contact between the skin and the electrodes. The displacement current travels through the clothing in between until reaching the electrodes. This way, we avoid the typical problems of long-term monitoring that can cause redness or swelling.

The goal is to build a prototype sensor capable of acquiring cECG and that is suitable to be installed in a piece of furniture. First, a series of tests will be carried out to characterize the size of the electrodes, the material of the electrodes, the material between the patient's body and the electrode, and the presence of moisture. Tests will be carried out in the laboratory with different circuits, and different insulation schemes, and tests will end up being carried out on humans with the best designed circuit, and with the electrodes that have had the best performance. By not requiring the patient to wear any type of sensorized gadget, nor requiring any action on the part of the patient to perform the recording, long-term adherence to the technological solution is improved.

2. Theoretical background

2.1 Anatomy of the heart

The human heart is a four-chambered muscle responsible for pumping blood throughout the human body. The heart is located in the chest's mediastinum, slightly off to the left of the chest's center (see Figure 2.1).

The pericardium, epicardium, myocardium, and endocardium are the four layers that comprise up the heart. The loose fibrous sac that surrounds the heart is called the pericardium. The pericardial space is the area between the pericardium and the epicardium, or outer layer of the heart muscle. The fluid in this area serves as a lubricant, preventing frictional damage to the heart while it is in operation.

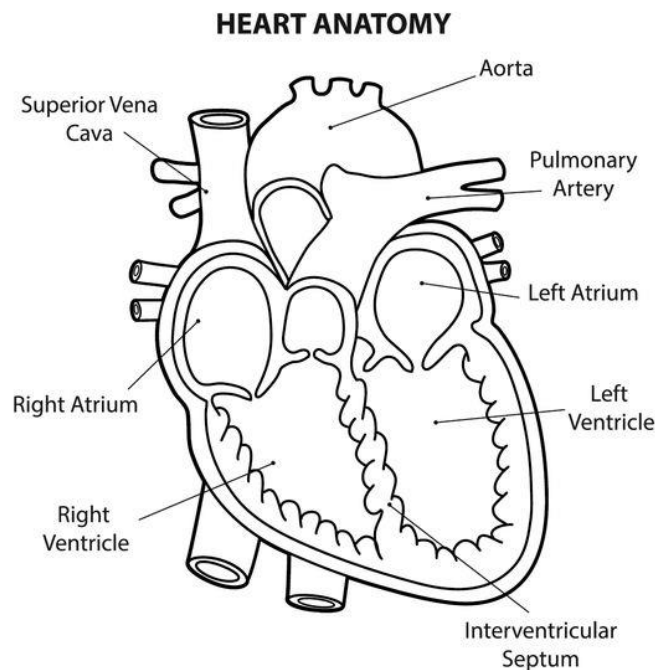


Figure 2.1 Anatomy of the heart [4]

The heart is divided into two sides, the right and the left. The right atrium (RA) and right ventricle (RV) are part of the right side of the heart. The left ventricle (LV) and left atrium (LA) are located on the left side. The atrial septum, located between the interventricular wall and the atria, anatomically divides the left and right sides of the heart. Like two distinct pumps that effectively operate independently of one another, these two sides of the heart function independently. The

inferior vena cava (IVC) and superior vena cava (SVC) carry blood from the body to the right atrium (RA) of the heart. The coronary sinus also empties into the right atrium, which receives the blood from the veins of the heart. Blood is forced into the right ventricle during diastole from the right atrium. After then, the blood is compelled to enter the pulmonary system, where it is given oxygen. The pulmonary veins carry oxygenated blood from the lungs to the left atrium. Blood flows into the left ventricle during diastole. The left ventricle circulates blood enriched with oxygen throughout the body.

Four valves in the heart allow blood to flow only in one direction. Blood cannot return to the cavities from which it originated when the valves are closed. The tricuspid valve divides the right atrium from the right ventricle, while the mitral valve divides the left atrium from the left ventricle. The left ventricle and the aorta are separated by the aortic valve. The pulmonary artery and the right ventricle are separated by the pulmonary valve [4].

2.2 The Cardiac Action Potential

The heart is a vital organ responsible for pumping blood throughout the body, and its function is finely regulated by the autonomic nervous system (ANS) to meet the varying demands of the body under different conditions. The ANS modulates the heartbeat through two primary branches: the sympathetic nervous system (SNS) and the parasympathetic nervous system (PNS) [5].

The action potential's shape significantly dictates how the cardiac rhythm and the heart's electrical impulse behave. On the other hand, cardiac cells are excitable. Tiny pores or channels in the cell membrane open and close in a stereotyped fashion when excitable cells are stimulated in the right way. Ions can move back and forth across the cell membrane when these channels open, which causes patterned changes in the transmembrane potential. The cardiac action potential is obtained by plotting these stereotypic voltage variations against time. As a result, the action potential represents the electrical activity of a single heart cell [6].

As we can see in Figure 2.2 the action potentials are divided into 3 phases, depolarization (0), repolarization (1 to 3) and the resting phase (4).

The phases of the action potential (see Figure 2.2):

0. Depolarization Phase: Sodium ions (Na^+) enter the cell through open sodium channels, causing a rapid increase in membrane potential.
1. Initial Repolarization: Potassium channels (K^+) open, allowing potassium ions (K^+) to flow out of the cell, which starts to bring the membrane potential back toward 0 mV.

2. Plateau Phase: The entry of calcium ions (Ca^{2+}) through calcium channels counterbalances the exit of potassium ions (K^+), resulting in a sustained depolarization known as the plateau phase.
3. Rapid Repolarization: Calcium channels close while potassium channels remain open, causing the membrane potential to return to approximately -90 mV.
4. Resting Phase: Both sodium (Na^+) and calcium (Ca^{2+}) channels are closed, and potassium rectifier channels remain open to maintain the membrane at a stable, negative resting potential.

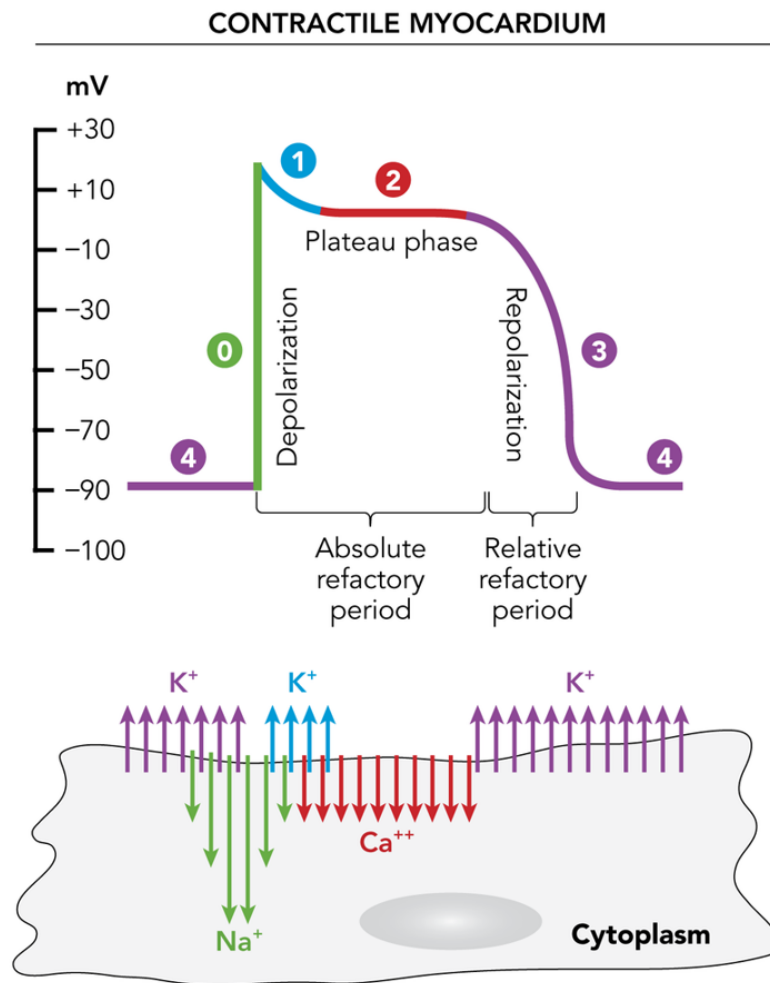


Figure 2.2 Cardiac Action Potential [7]

2.2.1 Depolarization

Depolarization is phase 0, which is essentially the onset of action potentials. Depolarization occurs when sodium channels in the cell membrane are stimulated to open. When this happens, positively charged ions enter the cell, causing a rapid change in the charge of the transmembrane potential. The potential that arises as a result of this rapid change is called depolarization. In cardiac electrophysiology, the heartbeat essentially refers to the depolarization phase.

Depolarization of one cell also causes neighboring cells to depolarize, because the momentary increase in voltage of the depolarizing cell causes sodium channels to open in neighboring cells as well. Thus, when a cell is stimulated to depolarize, a depolarizing wave is created that propagates throughout the heart, from cell to cell.

In addition, the speed of a cell's depolarization phase, which is shown by the slope of phase 0 of the action potential graph, explains how soon the next cell will be excited into a depolarization phase, thus determining the speed at which the electrical impulse propagates throughout the cell [7].

2.2.2 Repolarization

As the cell depolarizes, it cannot go into depolarization again until the flow of ions that occurs during depolarization is reversed. The process where the ions return to their original phase is called repolarization. Repolarization of cardiac cells corresponds to phase 1 through phase 3 of the action potential. Because depolarization cannot occur again until the repolarization phase is complete, the time from the end of phase 0 to the completion of phase 3 is called the refractory period. Because depolarization cannot occur again until the repolarization phase is complete, the time from the end of phase 0 to the completion of phase 3 is called the refractory period [7].

Repolarization of cardiac cells is a complex process that is difficult to be understood. The main ideas behind repolarization are simple:

- a) repolarization returns the cardiac action potential to the resting transmembrane potential,
- b) it needs time,
- c) the time is the width of the action potential and it is the refractory period of cardiac tissue.

2.2.3 Resting phase

Most cardiac cells, in the relaxation phase, are quiescent, as there is no movement of ions across the cell membrane. For some cells, however, the relaxation phase is not quiescent. In these cells, there is a leakage of ions to and from the cell membrane during the resting phase, in such a way that the transmembrane potential gradually increases. When the transmembrane potential is high enough, that is, when it exceeds the potential threshold, the appropriate channels are activated

and cause the cell to depolarize. This sudden activation of action potentials during phase 4 is called automaticity [7].

2.2.4 The cardiac dipole

In Figure 2.3 we can see the positive and the negative charges during depolarization and repolarization of the ventricles. The positive and negative terminals represent the cardiac dipole, records and it exists because there is a difference in charge between different areas of the myocardium. An ECG reports the orientation and magnitude of the cardiac dipole from several points of view. Compared with the Figure 1.1, we will say some information about the waves and the complexes of the heartbeat.

The P wave is indicative of atrial depolarization. If conduction is delayed, overlapping waves from both atria may seem notched. The small mass and delayed repolarization of the atria prevent apparent atrial repolarization. The QRS complex represents ventricular depolarization. The Q wave shows septal depolarization and appears in leads observing the heart from the left. The lead-dependent variation in the R and S waves reflects various cardiac dipole movements and perspectives. The T wave represents ventricular repolarization. The T wave is evident due to the bulk of the ventricles, even if repolarization is delayed. The upright T wave that we can see on the heartbeat, occurs because subepicardial myocytes, which have shorter action potentials, repolarize first, creating a similar charge distribution as during depolarization [8].

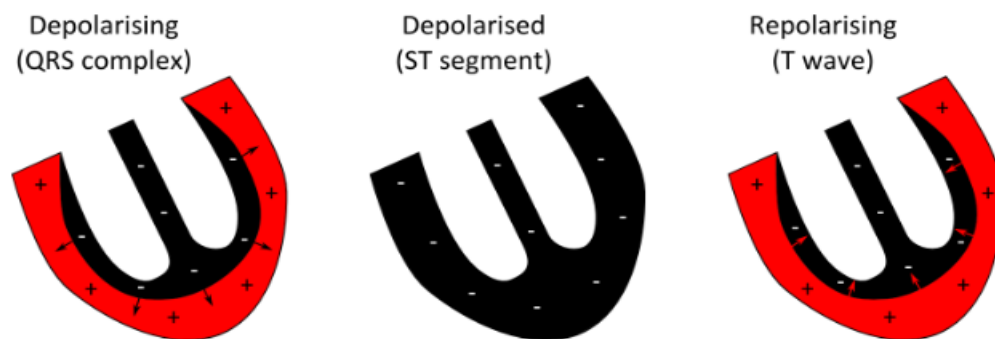


Figure 2.3 Positive and negative charges during depolarization and repolarization of the ventricles [8]

2.3 Einthoven ECG triangle

Willem Einthoven introduced the Einthoven Triangle, a key idea in electrocardiography (ECG). It involves the use of twelve limb electrodes. In order to create an imaginary equilateral triangle around the heart, three limb electrodes are inserted on the right arm (RA), left arm (LA),

and left leg (LL) (see Figure 2.4). Using this triangle, a reference system for calculating the heart's electrical activity can be established [9].

It has three standard limb leads:

- ⇒ Lead I: Measures the voltage difference between the negative electrode from the left arm and the positive electrode from the right arm.
- ⇒ Lead II: Measures the voltage difference between the negative electrode from the left leg and the positive electrode from the right arm.
- ⇒ Lead III: Measures the voltage difference between the negative electrode from the left leg and the positive electrode from the left arm.

According to Einthoven's rule, when the electric potentials of the two leads are known, the potential of the third lead can be calculated by summing the other two. This creates the triangle in the Figure 2.4.

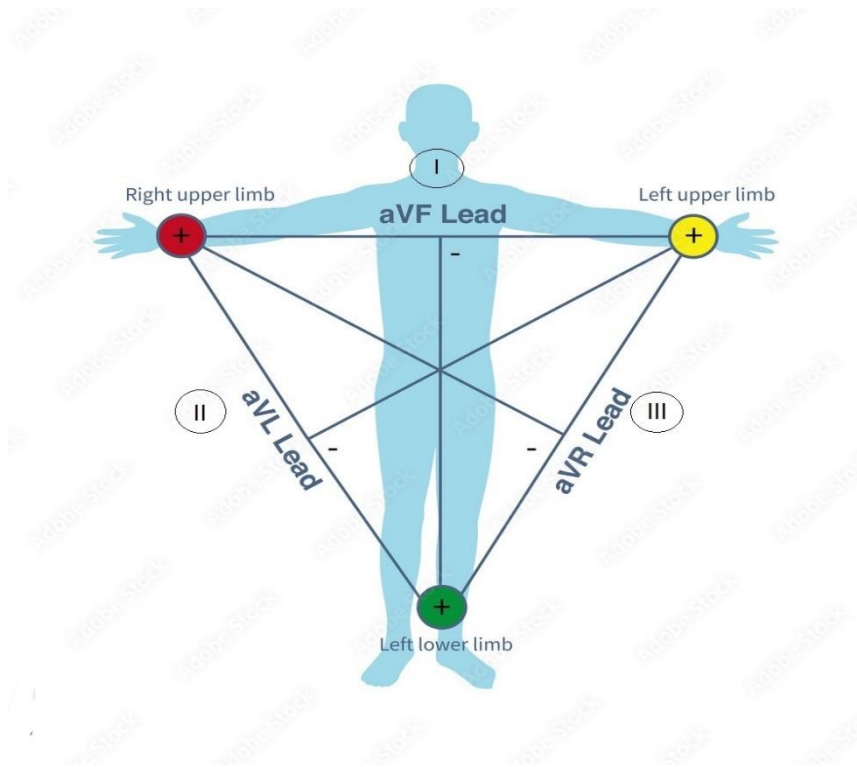


Figure 2.4 Einthoven ECG triangle [9]

2.4 Understanding the Electrocardiogram (ECG)

2.4.1 Principle of operation of ECG sensors

As we mentioned in 1.1, monitoring of electrocardiograms (ECGs) is a vital diagnostic technique for cardiovascular illnesses, offering useful knowledge into the rhythm and function of the heart.

The conduction of an electrocardiogram begins with the placement of electrodes on the limbs of the examinee, for higher accuracy. Electrodes can also be placed around the heart (precordial leads) to obtain additional information about the functioning of the heart muscle (for example, information about the ST segment in ischemic patients). Electrodes on the hands and around the heart detect the potential difference, while the electrode on the leg provides the ground and eliminates the common signal.

As we can see on Figure 2.5 the detected signal difference is amplified by an instrumentation amplifier and the new amplified signal pass through a filtering stage (Low-pass, high-pass and band-stop filters) to remove the noise and preserve the useful signal that is fed to an ADC unit for digitization. The digital signal is processed by a microcontroller and converted to an analog signal via a DAC stage.

Specifically, the electrodes record the difference in voltage due to the depolarization and repolarization of the muscles. The result of the electrocardiogram is displayed in a graph with the horizontal axis representing time and the vertical axis representing the difference in voltage detected by the electrodes. It is usually printed on paper or on the computer screen and can be a signal changing in the unit of time (the well-known cardiogram), a value (e.g. heart rate) or an alarm (e.g. tachycardia, bradycardia, fibrillation) [10].

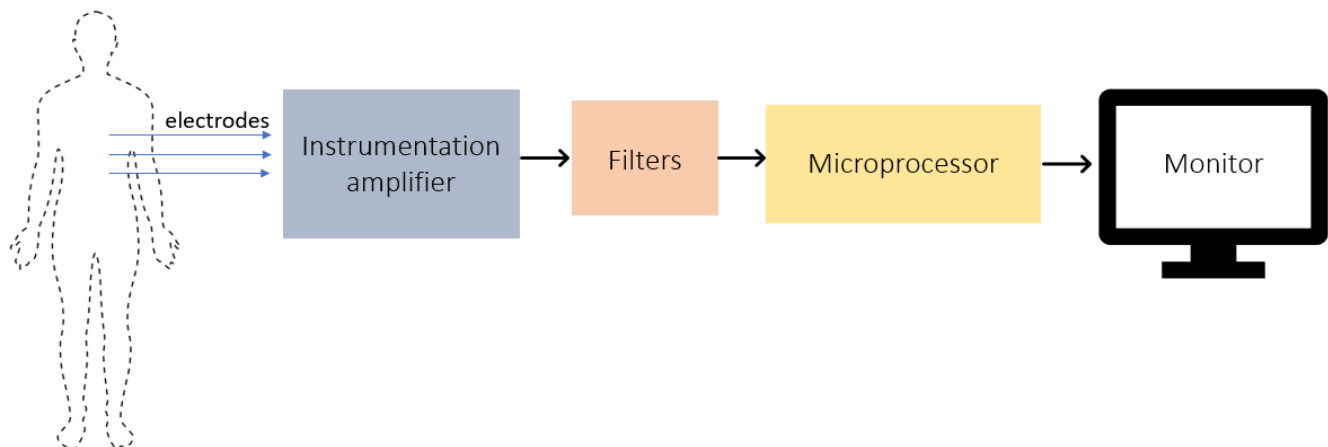


Figure 2.5 Block diagram of the ECG

2.4.2 Instrumentation Amplifier

The typical value of the ECG voltage is approximately 1mV (R wave width). This potential is a multiple of the potential of the electrode as well as other signals/interferences that are recorded such as the power supply signal of the electrical network at 50 Hz. The 50 Hz induced noise due to the mains power supply can be considered to be characterized by a capacitance of about 50 pF which translates into a resistance of about 65 MΩ. While a different ionic activity will prevail on the surface of each electrode due to the activity of the heart, the signal that will reach all the electrodes due to the mains voltage will be the same. So, if we could apply a process of subtracting the signals between the two electrodes, then the interference signal of the network would be zero. This brings us to the instrumentation amplifier (see Figure 2.6).

In the instrumentation amplifier all common signals that appear as noise at the ECG input can be considered as common signal at the amplifier inputs. For this reason, instrumentation amplifiers with a large CMRR are desirable in measuring weak signals, as they reject a significant percentage of common noise, thereby highlighting the useful signal [11].

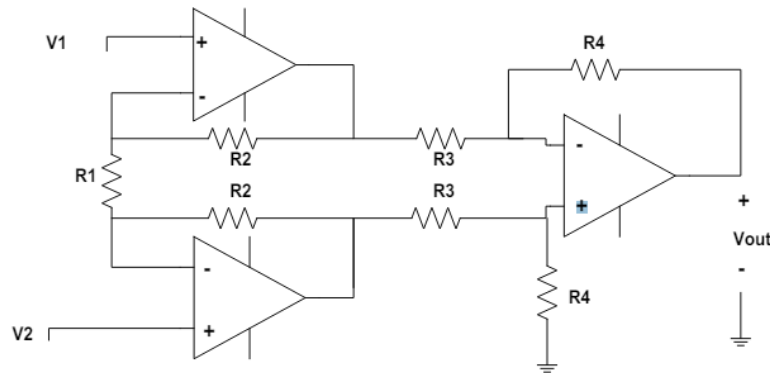


Figure 2.6 Instrumentation Amplifier

$$CMRR = \left| \frac{A_d}{A_c} \right| = 20 \log \left(\left| \frac{A_d}{A_c} \right| \right) \text{ dB} \quad (1)$$

$$V_{out} = \left(\frac{R_4}{R_3} \right) \left(1 + \frac{2R_2}{R_1} \right) (V_2 - V_1) \quad (2)$$

According to Equation (1) and (2) A_d is the gain of the amplifier and A_c is the common signal gain. A_c is zero, so the CMRR tends to infinity. CMRR on ECG is greater than 80dB.

2.4.3 Filters

In general, we can consider that there are three types of noise in the electrocardiogram.

1. **Baseline wander:** It is low-frequency noise caused by breathing, electrodes and patient movement.
For this noise we use a high-pass filter to cut off the low frequencies. The high pass filter cutoff frequencies above the cutoff frequency f_c , which is affected by the resistors and the capacitors. In many applications, 0.5 Hz is chosen as the cutoff frequency.
2. **Network interference 50Hz:** It is caused by the electromagnetic signals of the power lines present in the walls, floor and other electrical devices.
For this noise we use a bandpass filter that cuts off frequencies in a specific frequency band.
3. **Noise due to muscle movement:** It has several elements similar to those of the useful electrocardiogram. Muscle movements cause high frequency signals usually >100 Hz
For this noise we use a low-pass filter with a cut-off frequency of 100 Hz.

2.4.4 Protection Circuit

The protection circuit (see Figure 2.7) exists to protect a patient from possible currents that could threaten his life and injure him. Its purpose is to limit the current that will flow to the patient due to its connection to the ECG but also to cut it off if it exceeds the protection limits due to any malfunction. The value of the resistance R is a few $k\Omega$, in order to limit the current that will reach the patient in the event of a short circuit.

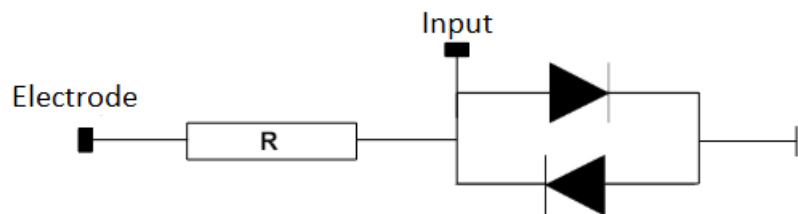


Figure 2.7 Protection Circuit

2.4.5 Interfacial electrochemical reaction

To convert ionic current into electron current, a process must occur at the interface between the electrode and the electrolyte to enable the flow of electric current. As illustrated in Equations (3) and (4), the electrochemical redox reaction system involves an electrode, with electrons on the left, and an electrolyte solution containing cations (C^+) and anions (A^-) on the right. During oxidation, metal C undergoes oxidation, dissolving into the electrolyte and releasing an electron to the electrode. Simultaneously, anion A^- is oxidized to a neutral atom, also releasing an electron to the electrode.

In the reduction process, cation C^+ gains an electron to form C, while A^- is regenerated from A. These reversible reactions are expressed as:



The current flows across the interface through the exchange of electrons during the redox reactions. When the current flows from the electrode to the electrolyte (left to right), oxidation predominates, whereas when the current flows in the opposite direction (right to left), reduction dominates. [12].

2.4.6 Electrodes

In the last few decades, a wide variety of biomedical electrodes have been developed and can be categorized based on many factors. They fall into the categories of resistive and capacitive electrodes based on material conductivity. From a function point of view, they can be classified as recording electrodes and defibrillation/pacing electrodes. Other classifications include flexible and rigid, as well as wet and dry.

Some of the most popular biopotential recording electrodes are:

- 1) Capacitive electrodes: They use dielectric materials to form a capacitive coupling to measure the potential change of skin. As we mentioned they are not suitable for long-term monitoring as they frequently result in skin irritation and discomfort for the patient.
- 2) Metal-plate electrodes: One of the most popular types of electrodes for biopotential sensing is the metal-plate electrode, which is made up of a metallic conductor in contact with the skin. The contact is made and maintained using a pad or gel that has been saturated with electrolytes.
- 3) Suction electrodes: One variation on metal-plate electrodes is the suction electrode, which holds in place without the need for adhesives or straps. Upon disengaging the bulb, the electrode adheres to the skin through suction. Only brief periods of time are permitted to use this electrode.

- 4) Floating electrodes: Floating electrodes are developed to reduce motion artifact.
- 5) Flexible electrodes: A flexible electrode has been developed to overcome fixed curvature of plate electrodes. One kind of flexible electrode is made of elastic, woven nylon fabric that has been coated with silver particles [12].

2.5 Non-contact ECG

Non-contact electrocardiograms, or NC-ECGs, are a state-of-the-art development in cardiac monitoring. They eliminate the need for conductive gels or adhesives to come into direct skin contact with the patient by using wearable technology, non-contact sensors, and complex signal processing algorithms to provide accurate and comfortable cardiac monitoring. By improving patient comfort, this technology is useful in clinical settings, home care and wearable health applications.

The aim of this part is to present the state of the art in non-conductive electrocardiogram (NC-ECG) technology, highlighting the latest advancements, key developments, and innovative applications.

2.5.1 Technological Developments and Innovations

ECG monitoring systems in the home environment are classified into telemonitoring, wearable continuous monitoring, and elderly and newborn monitoring.

Wearable non-contact ECG systems represent a groundbreaking advancement in the field of cardiac monitoring. These systems are designed to provide continuous and accurate monitoring of the heart's electrical activity without the need for direct skin contact, which enhances patient comfort and compliance.

Among the most notable developments in this area is the NCMB-Button, a wearable device integrated into everyday clothing that enables long-term monitoring of multiple biopotentials. The NCMB-Button, which has non-contact detection based on the ultra-high input impedance of the analog front end, can sense multiple biopotential signals, such as ECG, EMG, and EEG, through several layers of clothing without coming into direct touch with human skin [13].

Another development is the smart jackets designed for newborns. These jackets have built-in non-contact sensors that gently monitor the baby's heart, providing peace of mind to parents and healthcare providers without causing any discomfort to the little ones. For example, on the Eindhoven University of Technology [14] the smart jacket that they made contains the integration of conductive textiles for ECG monitoring and it is suitable for babies more than 25 weeks.

An example for elderly monitoring is the [15]. In this paper they created a fabric-sheet unified sensing electrode (FUSE) that can measure multiple biomarkers, like electrocardiogram (ECG), chest and abdominal respiratory movements (RMs), and ballistocardiogram (BCG). So, the patient just has to lay on the bed, and the fabric-sheet can measure every signal.

3. Material and Methods

3.1 Material

The main goal of this study is to design a capacitive coupled electrocardiogram sensor that can record cardiac signals through clothing and also to test Bitalino with capacitive electrodes and compare them. We are going to use Bitalino as a reference system. For the best results, both systems have been tested in direct contact with skin and through clothes. In this section we describe in detail all the equipment, techniques and experiments that have been used.

Usual ECG signals were acquired with a sample rate of 250 Hz [1]. Our final objective is a cECG, and that means that it has more noise and interferences than normal ECG. Because of that, we used higher sampling frequency to have better quality and to be able to filter the noise of the signal. So, we have used a frequency sampling of 1000 Hz.

The circuit that we have to build is based on a previous undergraduate thesis [16]. In that thesis, the student built a cECG sensor integrated into a chair. They used a pre-amplifier and a Sallen-Key lowpass filter with four resistors (68k Ω , 7 k Ω , 18 k Ω , 18 k Ω) and two capacitors (22nF and 222nF). With those numbers they had 104.38 Hz for cut-off frequency and 11 for gain (see Figure 3.1).

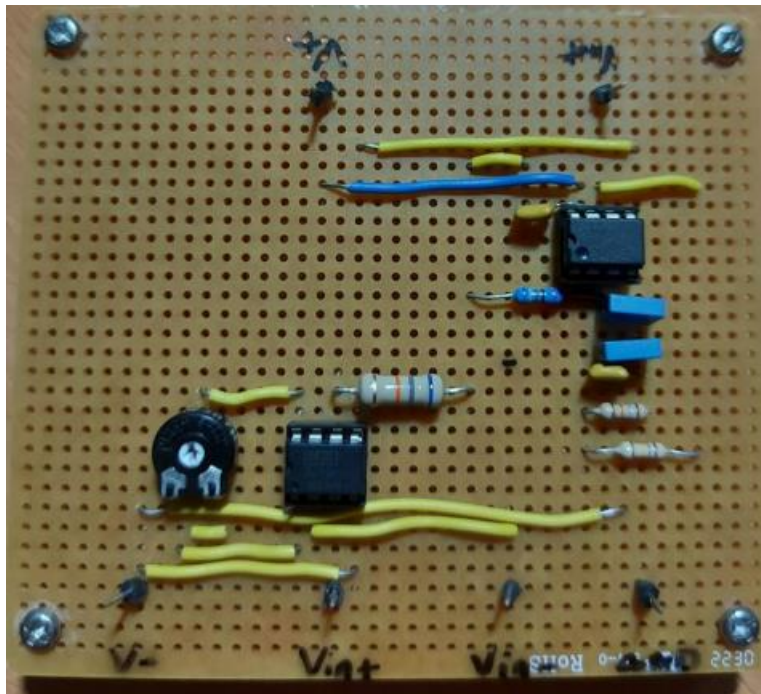


Figure 3.1 Circuit on Manuel's thesis [15]

The cut-off frequency can be reduced, because the goal is to have 30-40 Hz. The combination of a high gain with the values of the capacitors can turn the circuit into an oscillator. So, our goal is to fix the circuit and to build a cECG sensor integrated into a furniture (chair, bed or sofa).

3.1.1 Equipment

Some of the equipment we used includes:

1. For most of the experiments in this study, the device NI myDAQ (see figure 3.2) has been used. NI myDAQ is a low-cost portable data acquisition (DAQ) device that uses NI LabVIEW-based software instruments, allowing the user to measure and analyze real-world signals. It has analog input (AI) and output (AO), digital input and output (DIO), audio, power supplies, and digital multimeter (DMM) functions in a compact USB device. For that reason, it was useful for the digitalization the signal obtained with the custom-made sensor. We connect myDAQ with MatLab with the help of NI LabVIEW software. In APPENDIX 1 the code that we used on MatLab can be found.

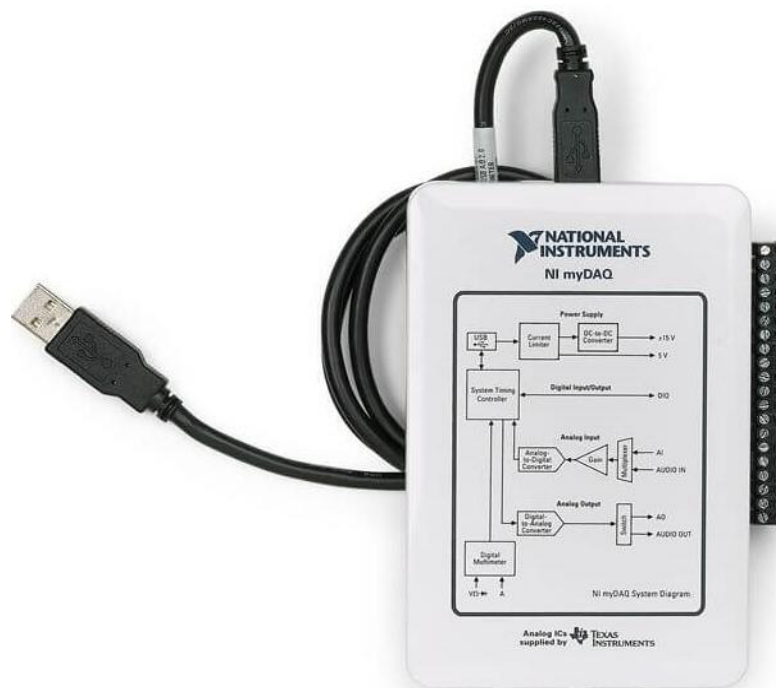


Figure 3.2 NI myDAQ device [32]

2. As we mentioned, we have used the Bitalino device in combination with capacitive electrodes. Bitalino is a commercial sensor that detects heartbeats and works with gel electrodes. So, we wanted to test how it will work with our dry capacitive electrodes. More specifically, we used Bitalino 4-Channel biosignalsPLUX (see Figure 3.3). It allows

wireless and high-quality signal acquisitions without limitations. It has four generic analog inputs and a 3000Hz sampling frequency.



Figure 3.3 Bitalino 4-Channel biosignalsPLUX [33]

3. In the calibration experiments we used a Function/ Arbitrary Waveform Generator (see Figure 3.4) which allows generating ECG signals with variable amplitude and beat rate. It has a bandwidth ranging from 1 μ Hz to 160MHz, and over than 140 different standard and arbitrary waveforms.



Figure 3.4 Function/ Arbitrary Waveform Generator

4. Moreover, we also used an oscilloscope (see Figure 3.5) for some of the experiments to make sure that our circuits work as they should. It has a bandwidth of 50 MHz, meaning it can accurately measure and display signals up to this frequency and a maximum real-time sampling rate of 1 GSa/s (giga samples per second), which ensures high-resolution signal acquisition.

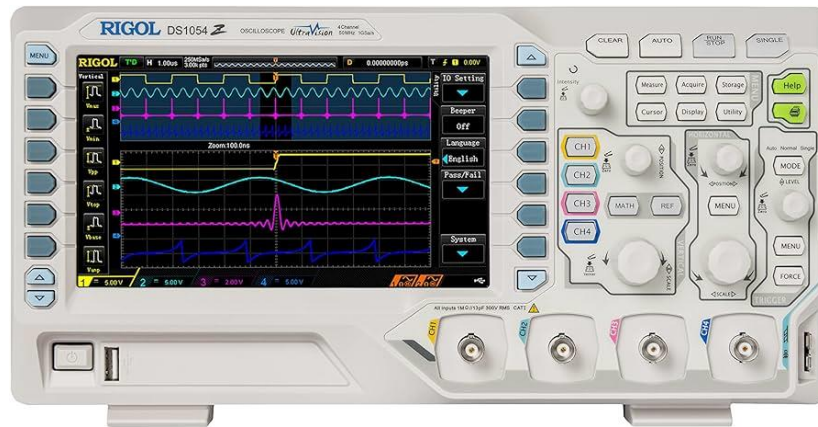


Figure 3.5 Oscilloscope [34]

5. We utilized TINA-TI software, developed by Texas Instruments. It is a powerful and user-friendly circuit simulation tool. We were able to design, simulate, and validate our circuit designs effectively before implementing them physically.
6. We have chosen to test two different types of conductive electrodes, a tape (Conductive Nylon Fabric Tape with conductive glue on the opposite side [17]) and a sheet (silver-plated nylon coated in a copper and tin [18]) (see Figure 3.6). Table 3.1 contains specifications for both of the conductive electrodes, like surface resistivity (Ohms/sq), temperature range ($^{\circ}\text{C}$) and thickness (mm).

Table 3.1 Specifications of the conductive electrodes

	<i>Conductive tape</i>	<i>Conductive sheet</i>
Surface resistivity	1.5 Ohms/sq	>1 Ohms/sq
Temperature range	-10 $^{\circ}\text{C}$ to 60 $^{\circ}\text{C}$	-30 $^{\circ}\text{C}$ to 90 $^{\circ}\text{C}$
Thickness	0.13 mm	0.11 mm

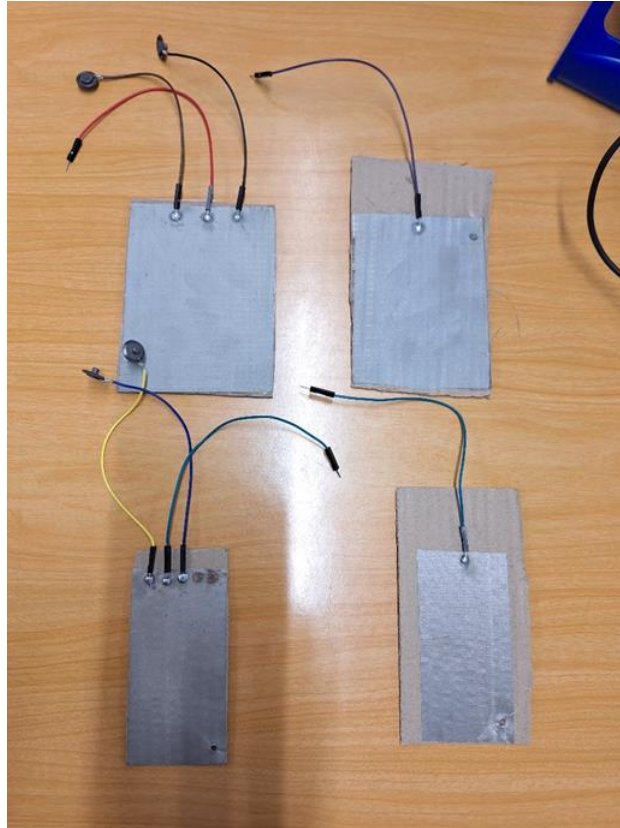


Figure 3.6 Custom-made capacitive dry electrodes

Table 3.2 contains the models and serial numbers of the equipment that was used during the study.

Table 3.2 Equipment

Equipment			
	<i>Kind</i>	<i>Model</i>	<i>Serial Number</i>
1	Digital Oscilloscope	Rigol DS1054Z 50MHz	DS1ZB204800569
2	POWER SUPPLY	FAC-662B PROMAX	FA662BE501
3	NI myDAQ	-	3019C62
4	Bitalino	4-Channel biosignalsPLUX	00:07:80:0F:30:08

Equipment			
	<i>Kind</i>	<i>Model</i>	<i>Serial Number</i>
5	Function/ Arbitrary Waveform Generator	PeakTech 4046	1CC041001
6	RS PRO Pocket Moisture Meter	RS-120	221120647

3.2 Methods

To test the custom-made circuit and the Bitalino, several implementations and setups were devised. These will be explored through the current section. We have elaborated Table 3.3 as an index for the whole section.

Table 3.3 Description of each implementation

	<i>Name</i>	<i>Materials</i>	<i>Results</i>	<i>Description</i>
1	BITALINO_SETUP	3.2.4	4.1.2	Experiment with the bitalino
2	CIRCUIT_SETUP	3.2.5	4.1.3	Experiment with the prototype circuit
3	CIRCUIT_SETUP_INSULATION	3.2.6	4.1.4	Experiment with the prototype circuit and insulation
4	CIRCUIT_SETUP_INSULATION_MOISTURE	3.2.7	4.1.5	Experiment with the circuit, insulation and moisture
5	BITALINO_SETUP_MOISTURE	3.2.8	4.1.6	Experiment with the bitalino and moisture
6	CIRCUIT_SETUP_INSULATION_2cm_ELECTRODES	3.2.9	4.1.7	Experiments with the circuit and smaller electrodes
7	CIRCUIT2_SETUP_INSULATION_REFERENCE	3.2.10	4.1.8	Experiments with the new circuit and insulation
8	CIRCUIT2_30_MINUTES	3.2.12	4.2.1	30 minutes experiment with the circuit2 and a volunteer
9	CIRCUIT2_VOLUNTEERS_MOISTURE	3.2.13	4.2.2	Experiment with circuit2, volunteers and moisture

3.2.1 The first circuit

This implementation is called `CIRCUIT_RAW_ECG`. In this section we will describe how we built the final circuit. On the first part of the circuit, we used an instrumentation amplifier INA128P to build the pre-amplification stage. We chose that amplifier because it has a low-power, general-purpose instrumentation amplifier that offers excellent accuracy [19]. This amplifier is embedded into a PCB board with a 10kΩ potentiometer, which is used to modify the gain according to Equation (5). (see Figure 3.7, red box).

$$G = 1 + \frac{50k}{R_g} \quad (5)$$

The potentiometer acts as the gain resistor (R_g) of the amplifier. According to the datasheet, the minimum gain for the amplifier is 1 without any resistor. We set $R_g = 10k\Omega$, so the minimum gain is 6.

The pre-amplification stage is crucial before the digitalization because we have a small amplitude bioelectric signal (ECG). Also, it can eliminate some types of noise but at the same time it can reduce the electromagnetic interference noise.

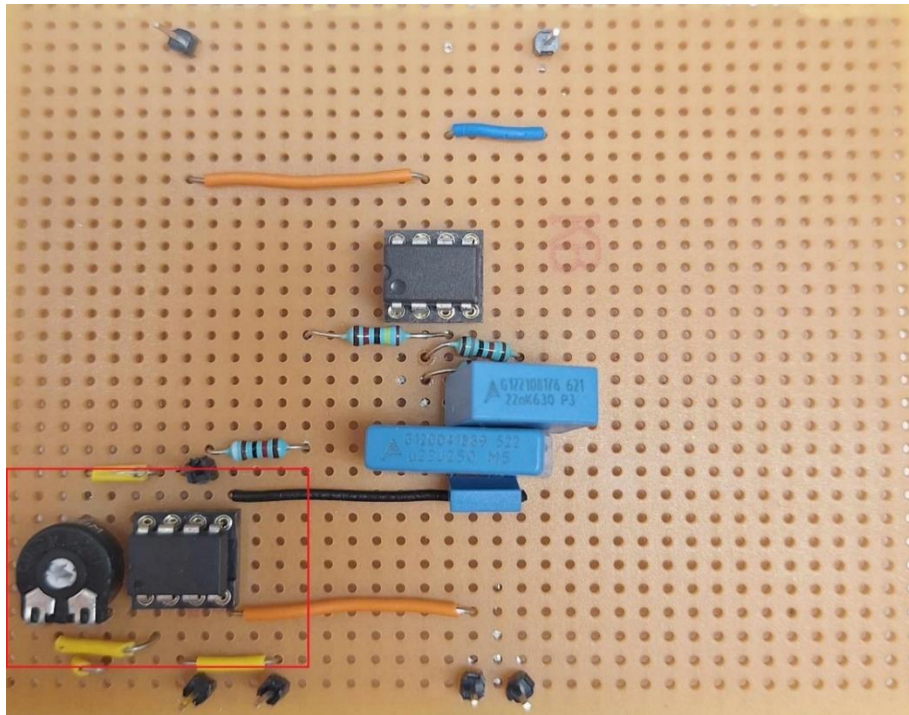


Figure 3.7 Circuit with a pre-amplifier and a Sallen-Key filter

The frequency spectrum of an electrocardiogram ranges from 0.05Hz to 100Hz [1]. The information of the QRS complex is found between 0.5-45Hz, but the most of the spectral power of the waves that make up the beat is between 5 and 15 Hz. For that reason and because myDAQ

doesn't include an antialiasing filter, we are going to use a low pass filter to eliminate the high frequency compounds before the digitalization.

Bioelectrical signals are characterized by their own low amplitude and the electrocardiogram signal is in the microvolt range. For these reasons, we decided to use a Sallen-Key lowpass filter with gain. It is easy to design while admitting extra gain (see Figure 3.8).

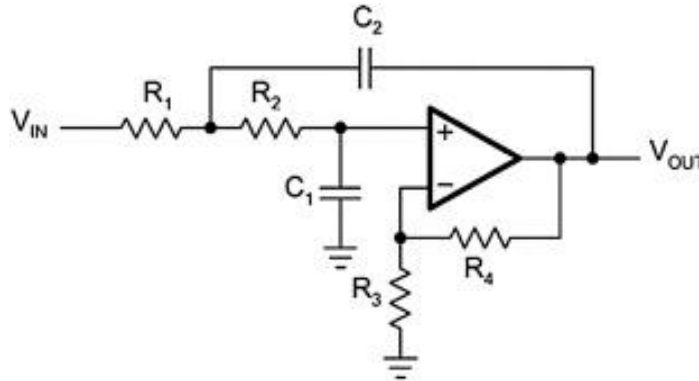


Figure 3.8 Sallen-Key gain Circuit

As we mentioned, the cut-off frequency that we want is $f_c=30-40$ Hz. Also, we decided to have a smaller gain (approximately $G=2.50$). With these data we found the appropriate values for the resistors and the capacitors based on Equation (6) and (7). Our goal was to find a combination of numbers that do not turn the filter into an oscillator.

$$f_c = \frac{1}{2\pi\sqrt{R1 * C1 * R2 * C2}} \quad (6)$$

$$G = \frac{R3 + R4}{R3} \quad (7)$$

Table 3.4 Components

Name	Value
R1	91kΩ
R2	24kΩ
R3	18kΩ
R4	27kΩ

<i>Name</i>	<i>Value</i>
C1	22nF
C2	322nF

With these components (see Table 3.4), the cut-off frequency of the low pass filter is 40.58 Hz and the gain 2.4.

We made the Block diagram of the circuit to understand more the flow of the system (see Figure 3.9). We used TINA-TI to simulate the circuit (see Figure 3.10) and to see how the signal responds to different frequencies (see Figure 3.11).

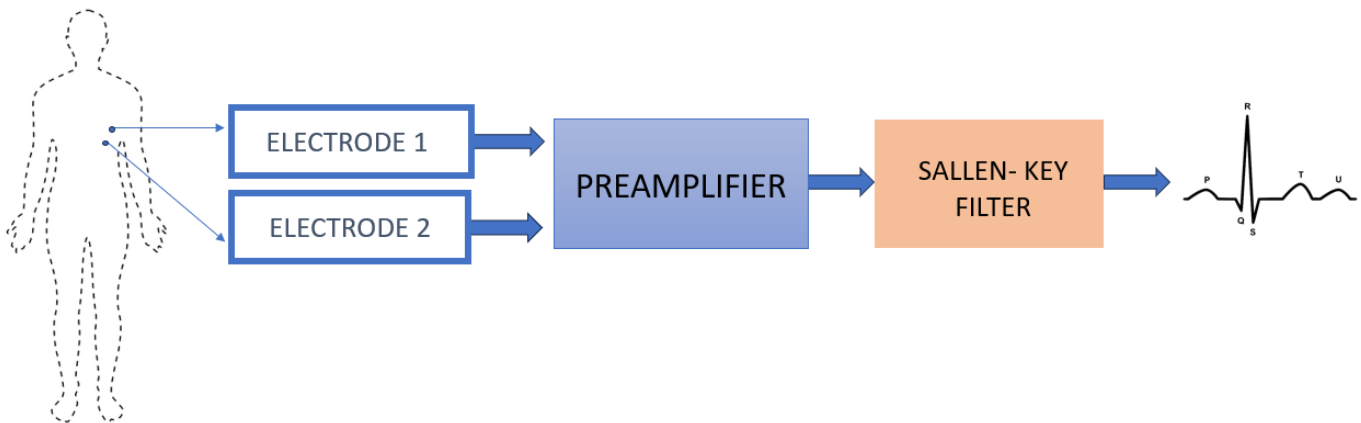


Figure 3.9 Block diagram of the circuit

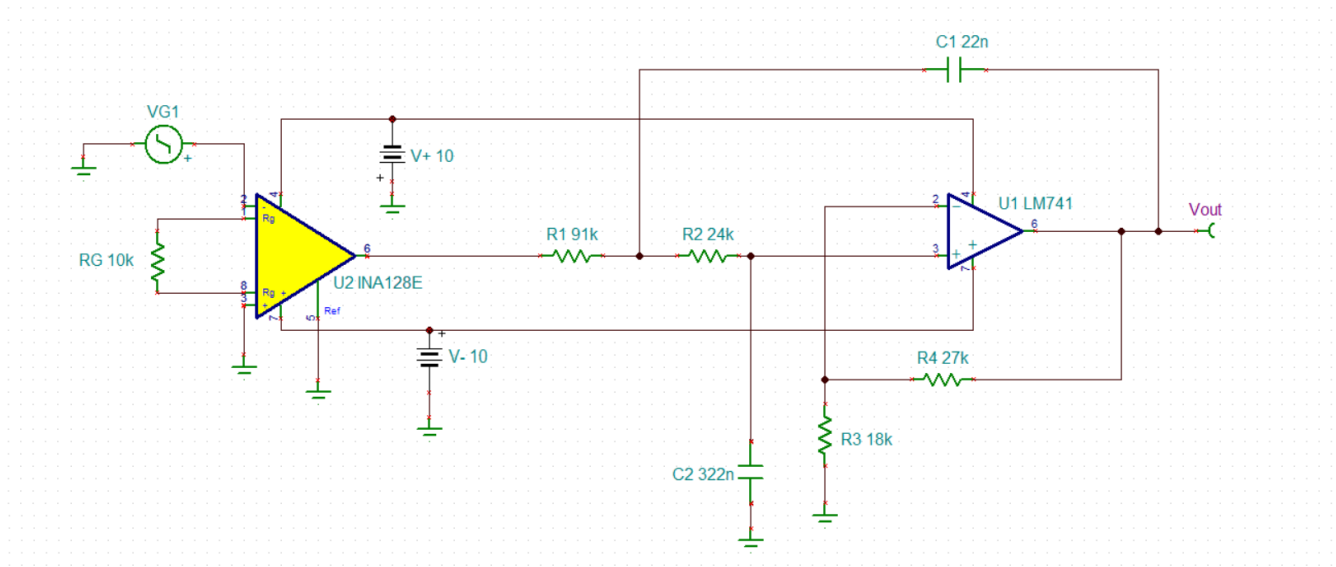


Figure 3.10 Schematic of the complete circuit

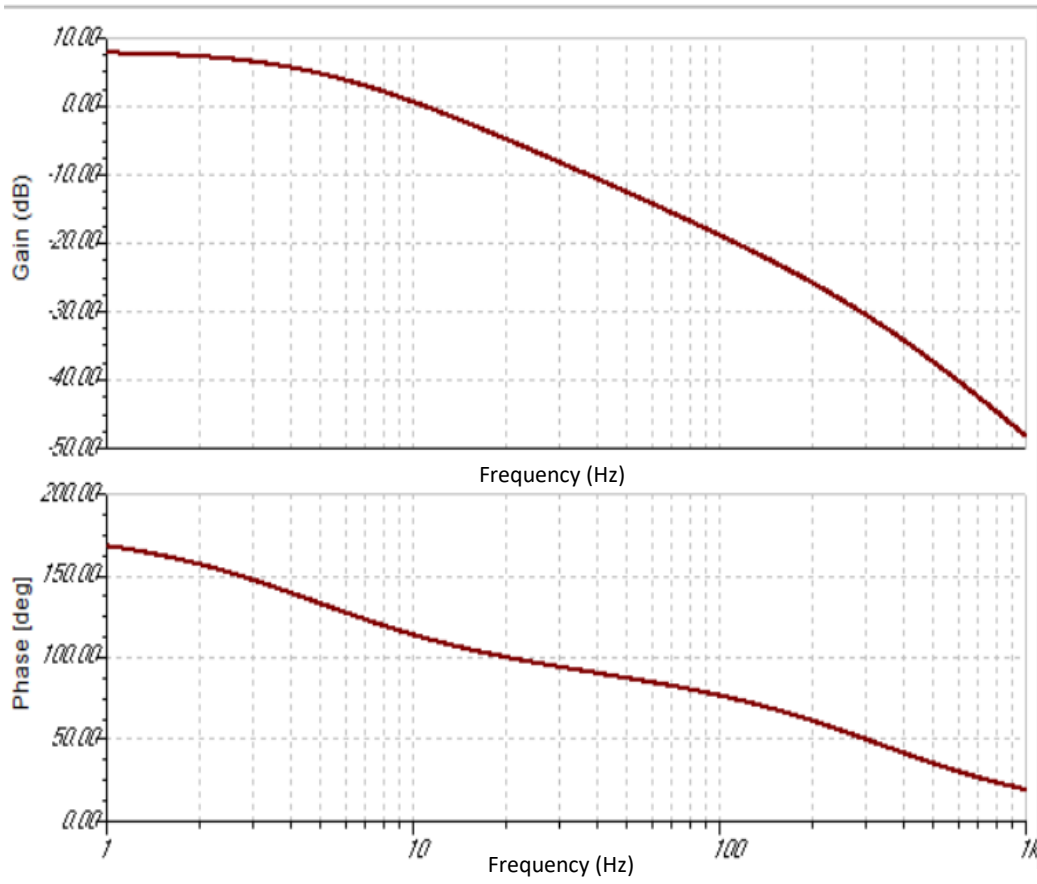


Figure 3.11 Transfer Characteristic Analysis

3.2.2 Acquisition using two electrodes with fingers

Before any other experiment we decide to test the circuit and the whole system with the help of oscilloscope and the power supply. Two conductive tapes are used as electrodes, and the index finger of each hand is touching each of the electrodes, so in this case the sensor is not capacitive (see Figure 3.12). The idea was to refine the quality of the fingers' signals and then move to more realistic placements.

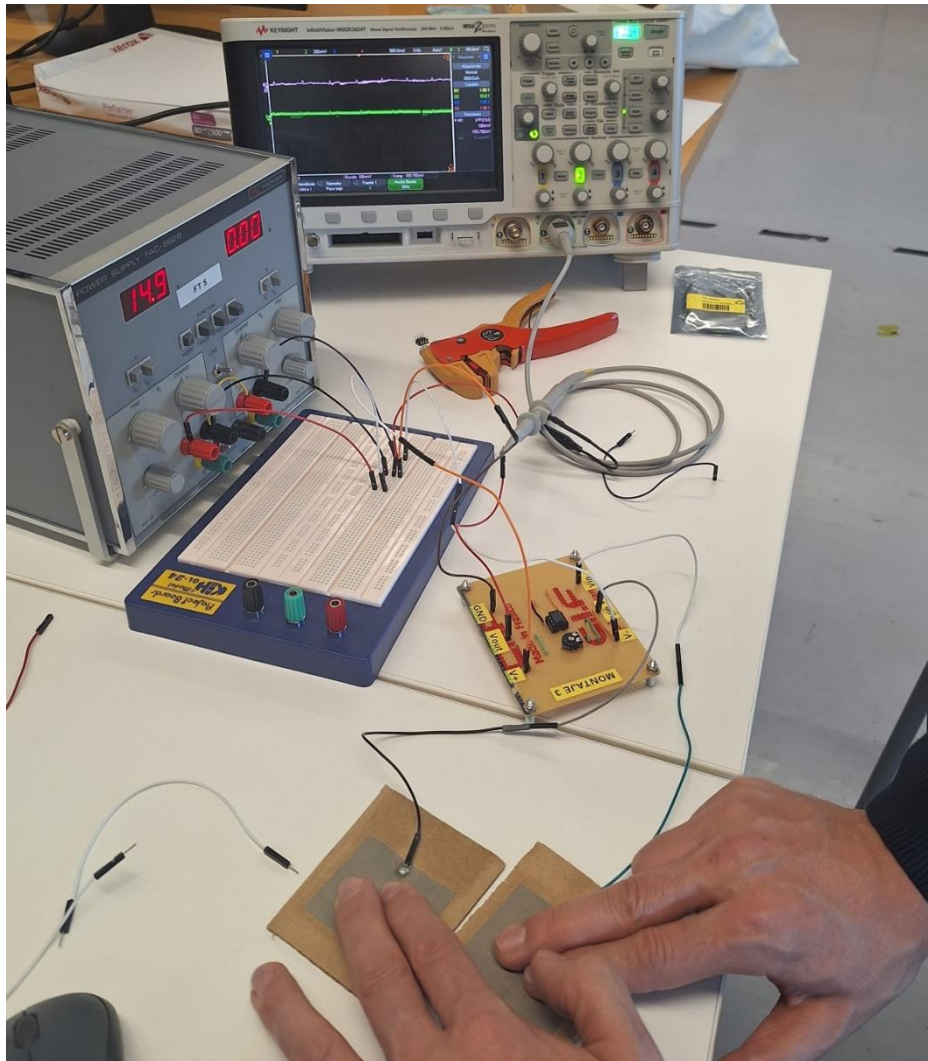


Figure 3.12 Experiment with fingers

3.2.3 Characterization of the conductive electrodes and of the materials

The conductive electrodes have attached wires that are connected either to the conditioning circuit or to the waveform generator. We decided that we want to test both electrodes, tape and fabric, in specific conditions and that simulate the coupling between the body and the electrodes through different materials with different signal amplitudes. We chose to use four different materials as dielectrics (see Table 3.5), a LDPE bag (Low Density Poly Ethylene), a A4 paper, a cotton t-shirt and a polyester t-shirt. Our purpose is to understand how our system and the electrodes work in different conditions. Also, for these experiments we used weight, because as we know, the pressure applied by the body is important between the electrode and the skin. So, we made the experiments without additional weight and with 1,2 and 5 kilograms, to see how they affect the signal.

Table 3.5 Dielectric constant of the materials

<i>Material</i>	<i>Dielectric constant</i>
LDPE bag	2.25 - 2.35
A4 paper	2.0 - 3.0
Cotton t-shirt	1.3 - 1.8
Polyester t-shirt	2.8 - 3.2

For the configuration of the experiments we built a set up (see Figure 3.13). It consists in a foamboard where we can pin one of the electrodes. We put the other electrode on top. The idea is

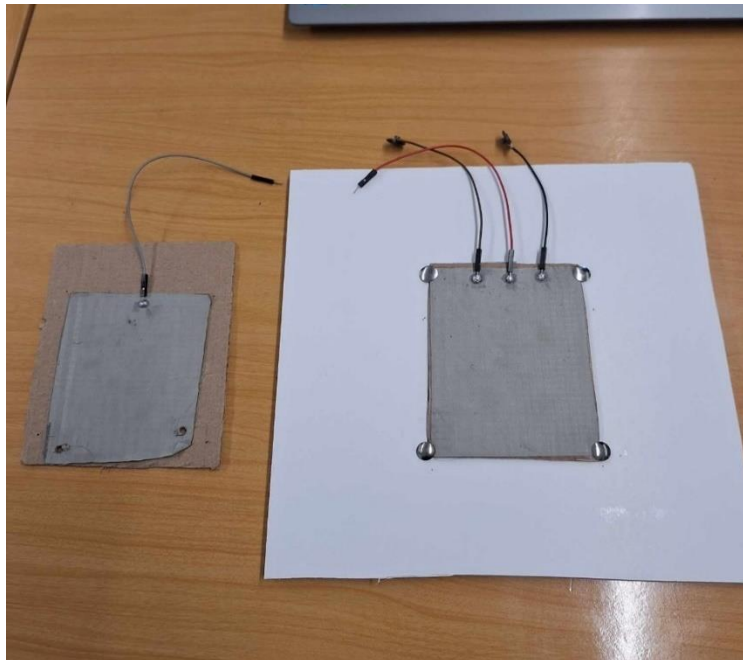


Figure 3.13 Set up

to connect the upper electrode with the signal generator and to touch the other electrode, so the upper side will be like the human body and the lower side will be the ECG electrode.

3.2.4 Experiment with Bitalino and the set up

This implementation is called BITALINO_SETUP. We decided to test the Bitalino first, so we can have a baseline to which we can compare the circuit. So, we connected Bitalino's leads with our electrodes and we used the OpenSignals application to record the signal. The reference electrode was disconnected without any signal (see Figure 3.14).

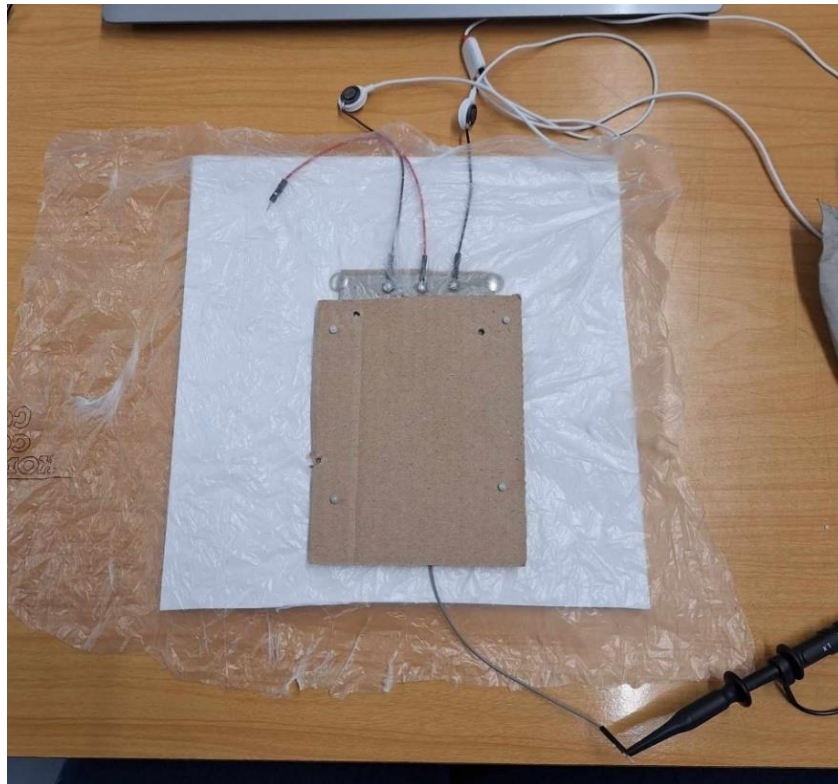


Figure 3.14 Bitalino experiment with plastic bag

3.2.5 Experiment with the circuit and the set up

This implementation is called CIRCUIT_SETUP. After testing the Bitalino, we continued with the circuit test. We put the circuit inside a metallic box for insulation. We connected the circuit with the myDAQ and the up electrode with the signal generator. Both grounds are connected using a prototyping board (see Figure 3.15).

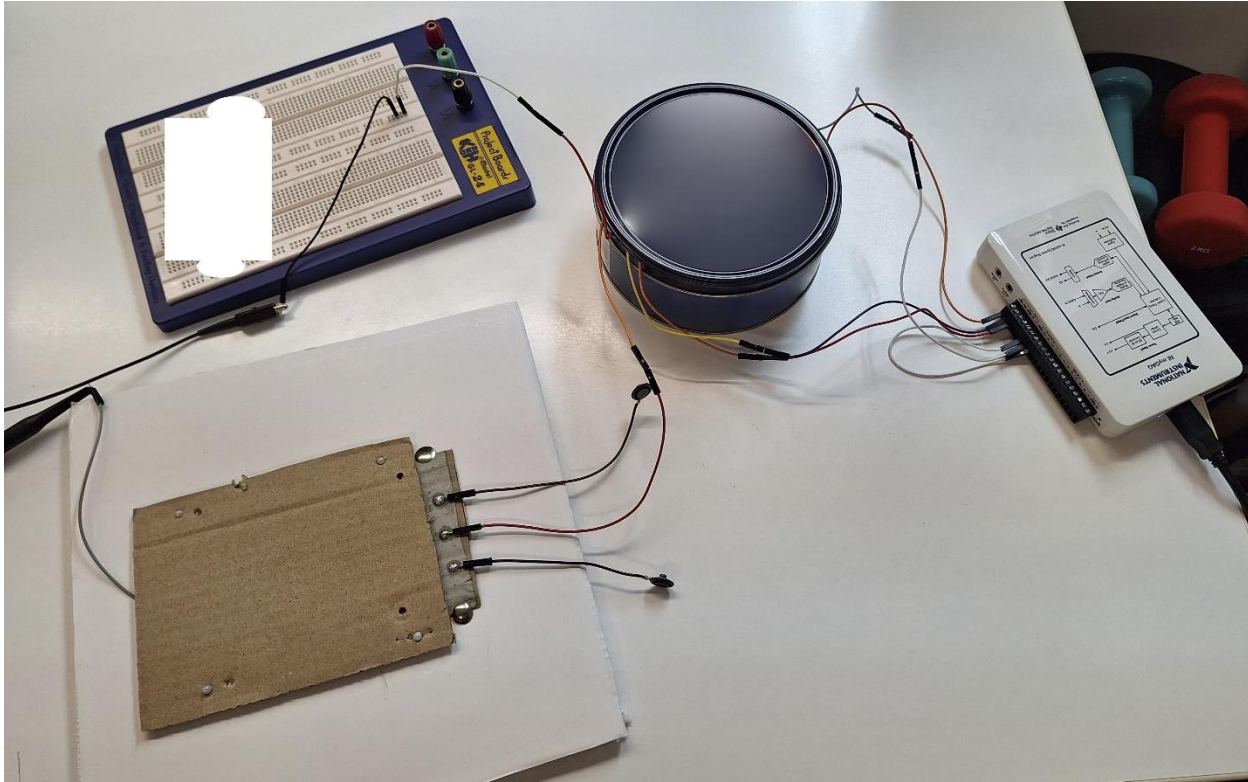


Figure 3.15 Circuit experiment with set up

3.2.6 Experiment with the circuit, the set up and insulation

This implementation is called `CIRCUIT_SETUP_INSULATION`. After the previous experiment we found out that our connections were noisy and the system needed insulation and shielding. For that, we put insulation tape in every connection of the wires, and we choose aluminum foil as a shielding method. We put aluminum foil on the input electrodes and the output wires (see Figure 3.16).

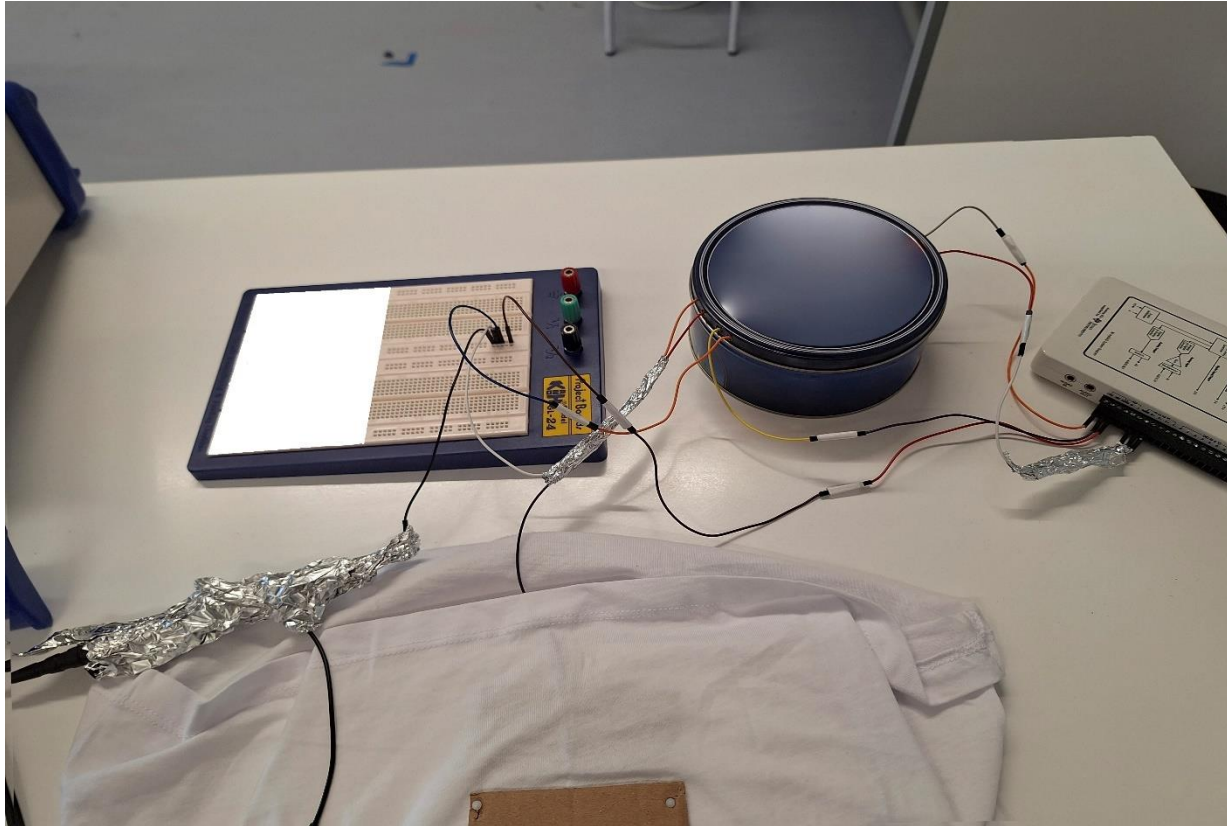


Figure 3.16 Circuit experiment with set up and insulation

3.2.7 Experiment with the circuit, the set up , insulation and moisture

This implementation is called `CIRCUIT_SETUP_INSULATION_MOISTURE`. Once we were able to obtain a clear signal, we want to see how our system will respond with different levels of moisture. It is well known that the level of moisture correlates with a better signal quality in non-contact ECG monitoring and when someone sweats a system with non-contact electrodes works better [20] .

Our set up now is the same as Figure 3.12 and the only thing that we changed was the moisture levels. We filled up a spray bottle with water and sprayed every material separately. To measure the moisture levels, we used the RS PRO Pocket Moisture Meter. This sensor is not calibrated to measure moisture in clothes but in materials such as wood, plasterboard and bricks. For this reason, the levels are relative to the ones measured without adding water. We set up the moisture in 0%, 10%, 20% and 30 %.

At this point we decided to use only the conductive tape because it seems that it works better for our system. In every experiment (see 4.1.1, 4.1.2, 4.1.3), we observe that the conductive tape works much better than the conductive sheet. We made the experiments without weights.

3.2.8 Experiment with Bitalino, set up and moisture

This implementation is called `BITALINO_SETUP_MOISTURE`. To compare the results from the implementation `CIRCUIT_SETUP_INSULATION_MOISTURE` we made the same experiments with the Bitalino. We used the set up from the Figure 2.10 and we took signals for every material and with a moisture level of 0%, 10%, 20% and 30%.

3.2.9 Experiment with the circuit, the set up, insulation and small electrodes

This implementation is called `CIRCUIT_SETUP_INSULATION_2cm_ELECTRODES`. The reason behind this implementation is the fact that the electrodes in an ECG are small, compared to the ones we had been testing, and in real life they should fit on top of the body. So, we made new electrodes, $2\text{cm} \times 2\text{cm}$, to test the circuit again and see how the difference in the size of the electrodes can affect the signal.

3.2.10 The final circuit

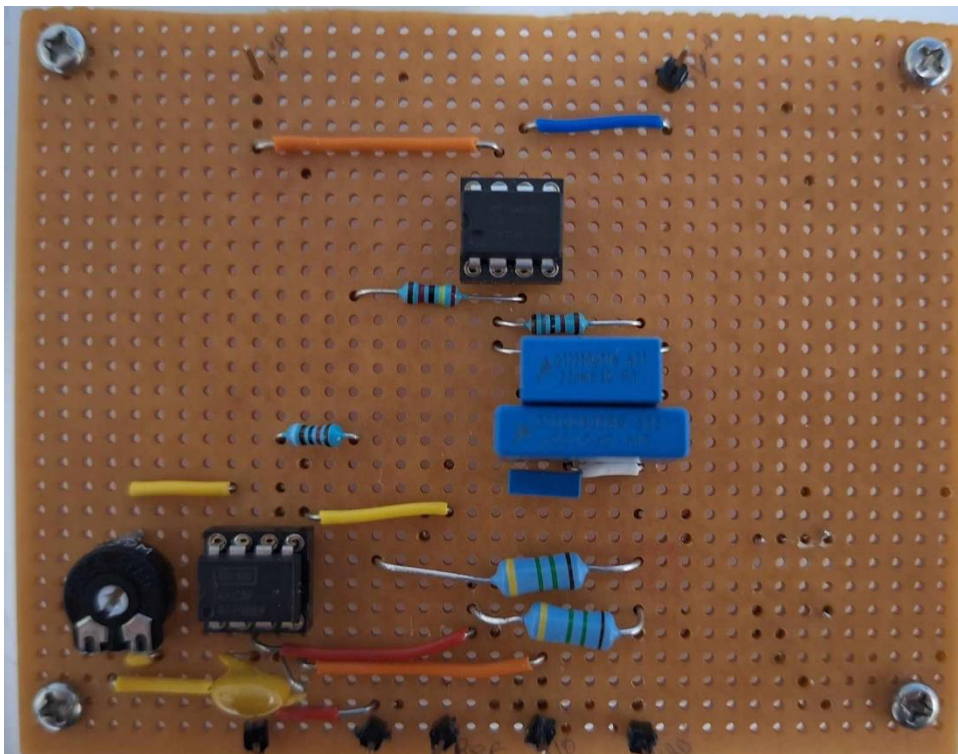


Figure 3.17 Final circuit with pre-amplifier, Sallen-Key topology filter and high valued resistors in series with this capacitor

This implementation is called `CIRCUIT2_SETUP_INSULATION_REFERENCE`. After the previous experiments we understood that we need to improve the signal integrity. For that we made

a new circuit. We used the same components as the first circuit but now we added some new components on the input. The first difference is the reference electrode.

As we found in the literature [21] a high valued resistor (few $M\Omega$), connected to ground, in series with a capacitor (same as the capacitance of the cotton t-shirt), forms a passive high-pass cell at very low frequencies (of about 1 Hz). For that reason, we added two resistors of 1.5 M Ω each and a 180pF capacitor in series with them. Every resistor is connected with the ground and with one of the inputs (see Figure 3.17). So, we repeated the same experiments with the two different t-shirts.

3.2.11 Set up for experiments with volunteers

To measure real ECG signal from volunteers we needed a new set up. For that reason, we built the following set up (see Figure 3.18, on the left the schematic idea, on the right the real chair). We used a chair and we put a 3 cm foam layer to create a soft seat for the electrodes. We added the foam because we observed that the hard surface of the chair caused the electrodes to deform, preventing perfect contact with the patient's body when they sat down. So, we reduced this deformation, ensuring that the patient's body applies perfectly to the electrodes. We put the electrodes next to each other and the reference electrode on the edge of the foam. We put aluminum foil in every connection and wire for shielding.

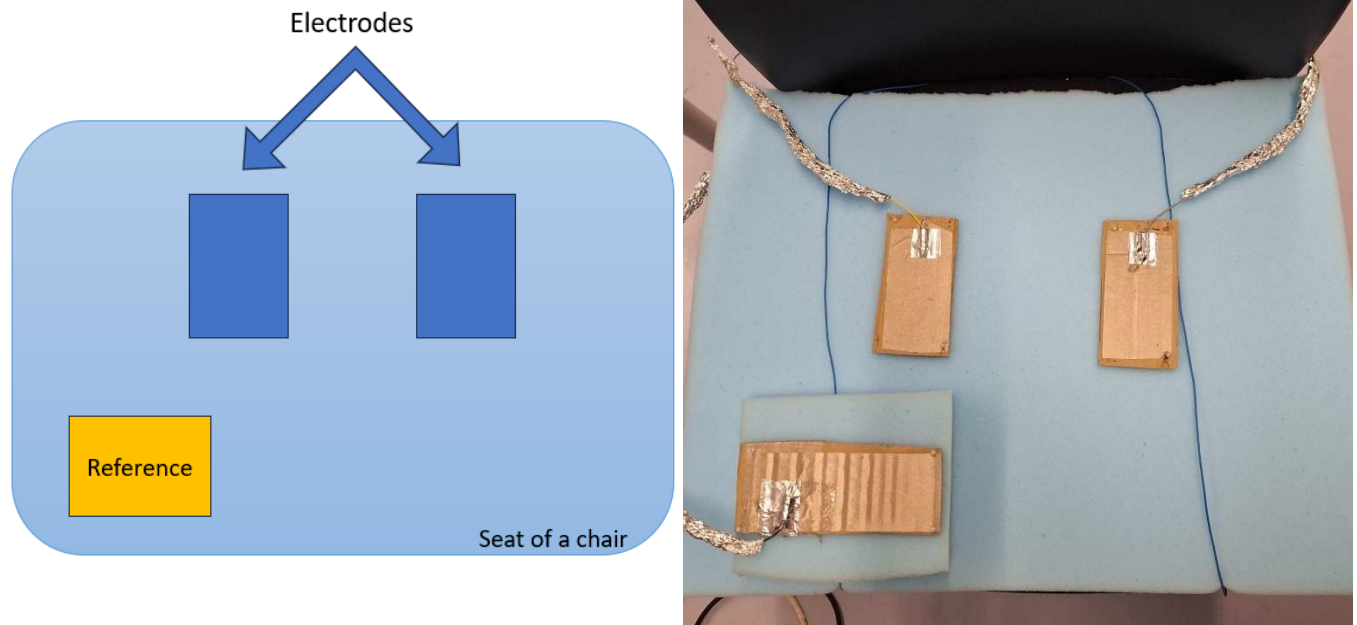


Figure 3.18 Set up for experiments with volunteers

As we mentioned before, the moisture plays an important role in the recording of the signal. The experiments took place in June, which means that the weather was hot and most of the volunteers were more likely to sweat. We noticed that when the person was sweating, the signal quality was much better.

We decide to make two different experiments. The first one is a recording for 30 minutes. Since we know that the sweat increases when sitting for a long time, we recorded an experiment with one volunteer on a longer period (30 minutes).

Since we noticed how the moisture affects the signal, we decided to divide the second experiment into two parts. First, we took the signal without excess moisture and secondly, we added a little moisture with the spray bottle, which applied once (as the moisture test in 3.2.6, 3.2.7) above the electrodes to see if our claim is indeed valid.

We must emphasize that all the experimental procedures were approved by the Ethics Committee of the Universidad San Pablo-CEU. All the volunteers provided informed consent prior to participation in our experiment.

3.2.12 30 minutes experiment with the circuit2 and a volunteer

This implementation is called `CIRCUIT2_30_MINUTES`. As we mentioned and in 3.2.10, we decided to make a 30 minutes experiment with one volunteer to see how the quality of the signal will changed through the time. The subject just sat on the chair and didn't change position for 30 minutes (see Figure 3.19).

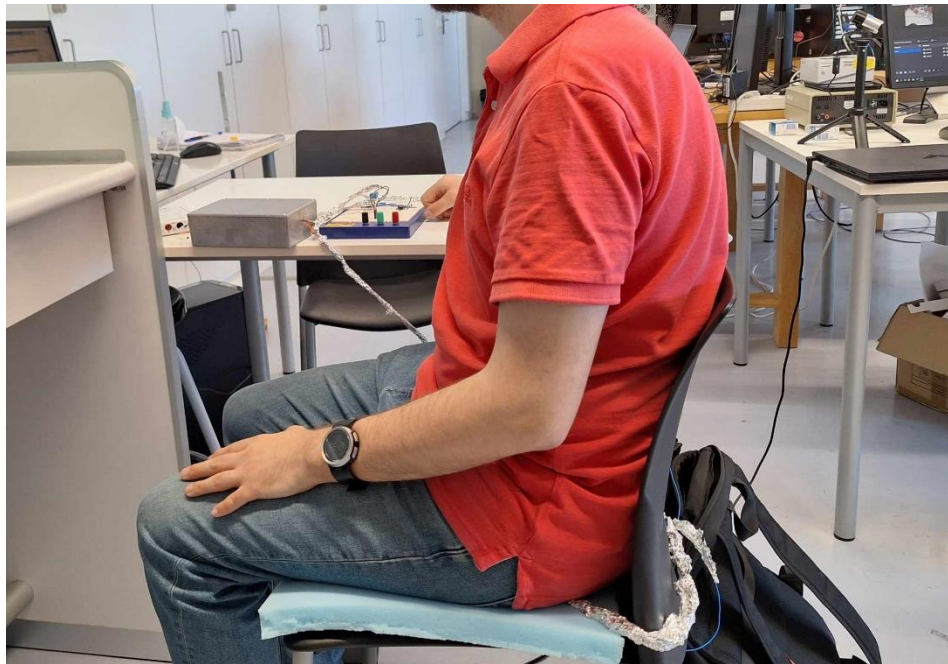


Figure 3.19 Experiment implementation

3.2.13 Experiment with circuit2, volunteers and moisture.

This implementation is called CIRCUI2_VOLUNTEERS_MOISTURE. As we mentioned in 3.2.10, we decided to divide the second experiment into two parts. First, we took the signal without excess moisture and secondly, we added a little moisture above the electrodes to see if our claim is indeed valid.

Our proposed system was validated through experimental measurements of 8 healthy people, 4 males and 4 females (20-43 years old, 1.66-1.82 m height, 55-110 kg weight). Each experiment was performed for 1 minute and the subject just sat on the chair without moving.

To evaluate prototype quality, the mSQI method was employed, calculating various features for each 5 second window of ECG data. These features include kSQI for artifact identification, pSQI for spectral power comparison, cSQI for R-R interval variability, basSQI for baseline drift, and dSQI. Each feature is assessed using a fuzzy possibility distribution, yielding values between 0 (unusable signal) and 1 (perfect signal), which are then aggregated using a geometric mean [22]. This method previously showed a 98% agreement with ECG quality labels in a Computing in Cardiology Challenge dataset [23].

It is important to note that this algorithm has previously only been applied to contact electrocardiograms. This will be the first instance of its use with non-contact ECG signals.

So, we used this algorithm to see how the signals without and with moisture worked, and in which one we can detect the most R-peaks.

3.2.14 Signal Processing

In this study we are building a building a prototype system on breadboard, so we expect the signals to contain much more interferences than in a clinical environment. Especially, the cECG signals

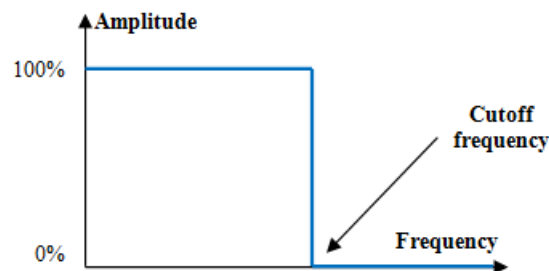


Figure 3.20 High-pass filter [28]

contain a lot of network noise. For this reason, we are going to apply three filters in the MatLab environment.

The first one is a High-Pass Filter (see Figure 3.20). It is an EQ curve that is used to remove low-frequency sounds from an audio signal. It is called a high-pass filter because it allows high-frequency signals to pass through, while attenuating (reducing the amplitude of) lower-frequency signals. We used it because we wanted to remove the baseline wander. We chose as a cut off Frequency 1 Hz. This means that frequencies below 1 Hz are attenuated, effectively removing baseline wander.

The second is a bandpass filter (see Figure 3.21). A bandpass filter is an electronic circuit that allows a specific range of frequencies to pass through while attenuating frequencies outside that range. We chose as a low cut off Frequency 1 Hz, to ensure that the baseline wander and other very low-frequency noises are removed, and as a high cut off Frequency 40Hz ensure that the important components of the ECG signal, such as P-waves, QRS complexes, and T-waves, are preserved.

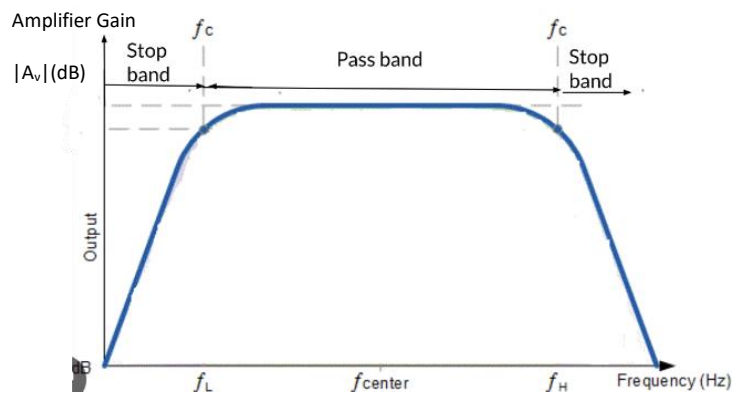


Figure 3.21 Bandpass filter [30]

The third and last filter is a notch filter to eliminate network noise (see Figure 3.22). The power network interference appears at 50Hz, and its harmonics can also manifest at $k \times 50$ Hz. Notch filter is a type of narrow band stopband that attenuates frequencies at 50Hz. We choose two cut off frequencies [40 60] Hz. This creates a notch filter that attenuates frequencies between 40 Hz and 60 Hz.

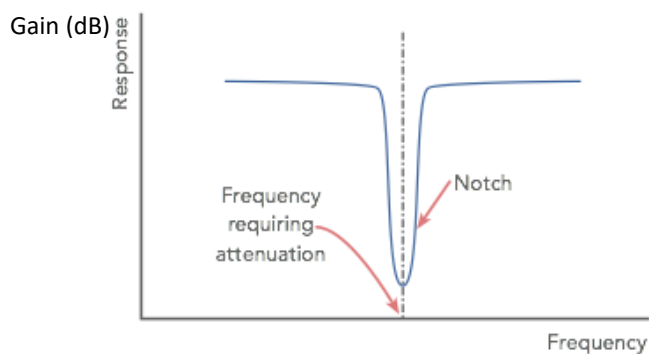


Figure 3.22 Notch filter [29]

By carefully selecting these cutoff frequencies, you ensure that the filters effectively remove unwanted noise while preserving the important features of the ECG signal, leading to more accurate and reliable analysis.

4. Results

4.1 Results for the calibration experiment

4.1.1 Acquisition using two electrodes with fingers

In the figure 4.1 below we can see the signal that we took with the help of the oscilloscope and the fingers on the electrodes. It is clear that we can see heart beats, before (green signal) and after (white signal) the filter of the oscilloscope. So, after that experiment we can continue with the others and test our system with non-contact electrodes.



Figure 4.1 Signal in the oscilloscope

4.1.2 Results for Bitalino with setup

Results from the implementation BITALINO_SETUP. In the tables below, we will present the results of the experiments. The amplitudes are the lowest for every case where we can observe R peaks. On table 4.1 we can see the results from the experiment with the conductive sheet and on table 4.2 we can see the results from the experiment with the conductive tape.

Table 4.1 Bitalino with set up results-Conductive sheet (output voltage measurements with various materials and weight values)

	PLASTIC BAG	A4 PAPER	COTTON	POLYESTER
Without weight	4V	5V	5V	5V
1kg	3V	4V	4V	4V
2kg	2V	3V	3V	3V
5kg	1V	1V	2V	2V

Table 4.2 Bitalino with set up results-Conductive tape (output voltage measurements with various materials and weight values)

	PLASTIC BAG	A4 PAPER	COTTON	POLYESTER
Without weight	4V	3V	4V	3V
1kg	3V	2V	3V	2V
2kg	2V	1V	2V	1V
5kg	1V	0.5V	1V	0.5V

It is clear that the conductive tape seems to work better than the conductive sheet. Nevertheless, the amplitude is really high. The noise in the frequency range of the ECG, 0.05 – 100 Hz, is masking part of the signal. So probably the Bitalino is not suitable for these kinds of experiments and for contactless ECG. Even with that big amplitude the noise is really big and we can barely see the R-peaks (see Figure 4.2).

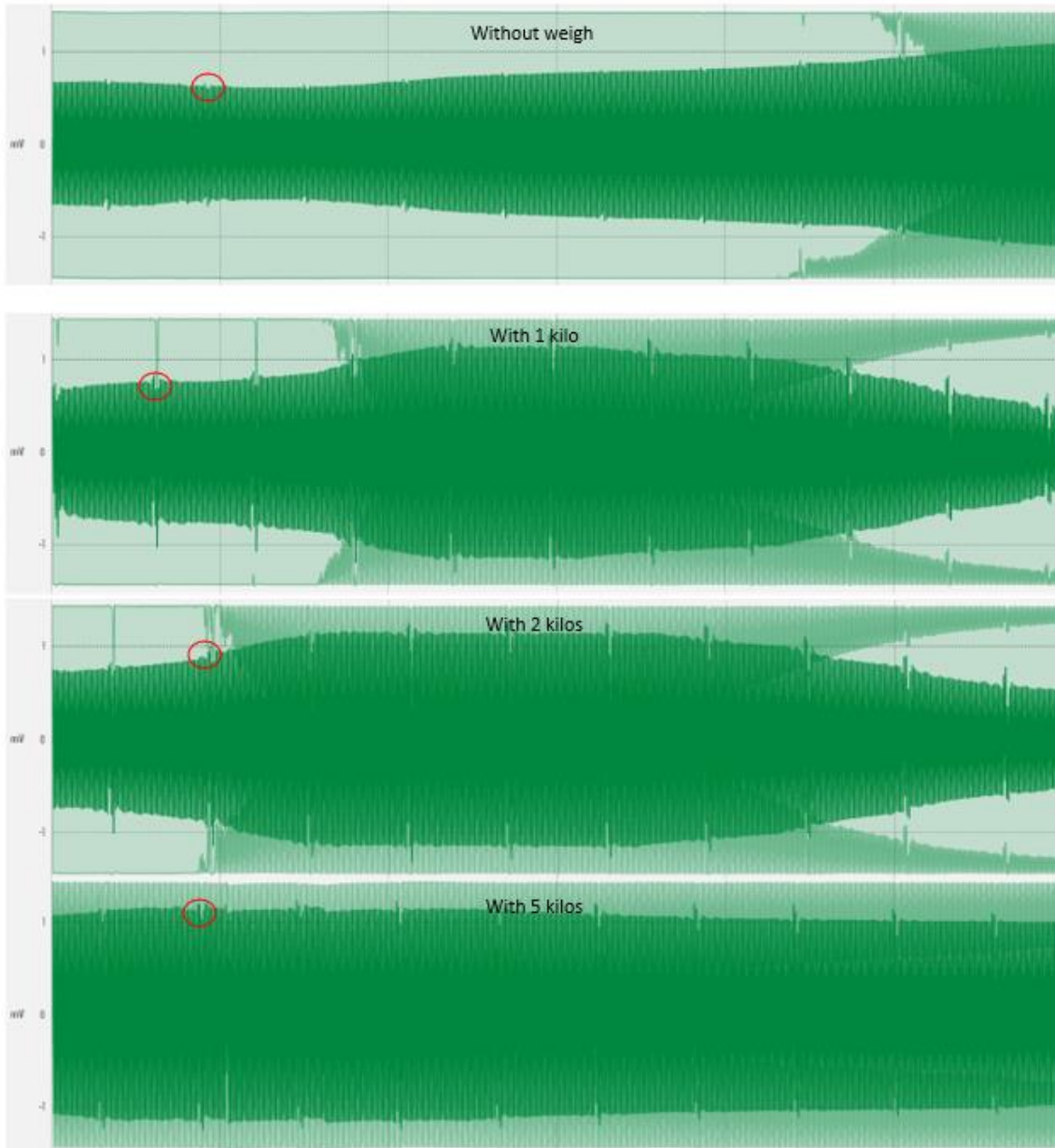


Figure 4.2 Signals of experiments with bitalino, set up and cotton t-shirt (mV/s)

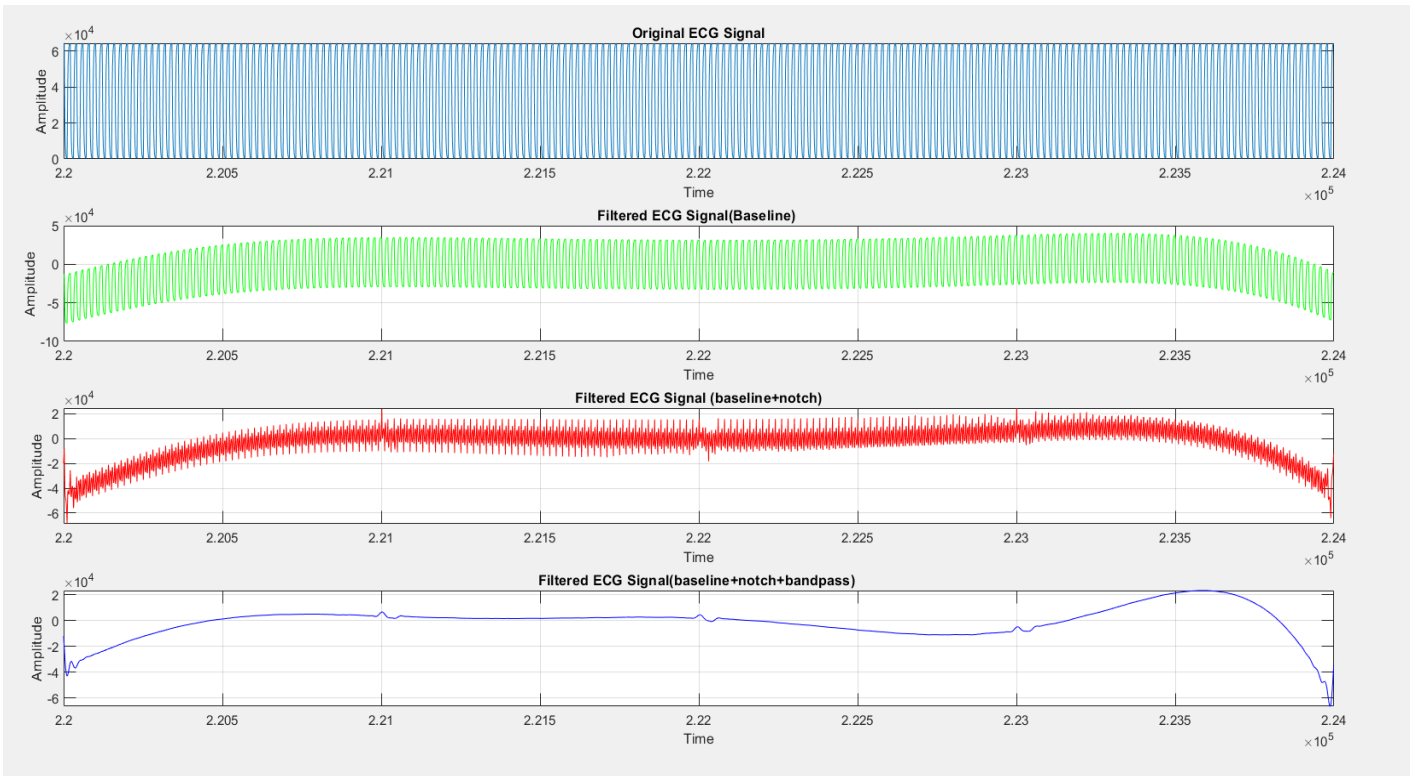


Figure 4.3 Filter signal of experiment with the Bitalino, set up and cotton t-shirt with 5 kilograms (mV/s)

In Figure 4.3 we can see a subplot of the filter signal using cotton t-shirt with 5 kilograms. The first plot is the original signal for the cotton t-shirt without weight, the second plot is the same signal with a high-pass filter, the third plot is the same signal with a high-pass and a notch filter and the last one is the same filter but with a high-pass, a notch filter and a bandpass filter. We can clearly see how every filter affects the signal. The last one is a clean signal, with less noise, where we can detect the R-peaks.

We can see that the x and y axis are not correct. This happened because the file with the signal from Bitalino is has samples and no seconds. For that, the time axis is 220.000, which means the 3.6th minute of the recordings ($220.000/1000=220$, $220/60=3.6$ minute). So, in this Figure we can see the first 4 seconds from the 3,6th minute. This Figure is showing the ADC conversion values without having been translated back to physical units. The data was represented as a 16-bit integer, hence the scale value.

4.1.3 Results for circuit with set up

Results from the implementation CIRCUIT_SETUP. In the tables below, we will present the results of the experiments. The amplitudes are the lowest for every case where we can observe R peaks. On table 4.3 we can see the results from the experiment with the conductive sheet and on table 4.4 we can see the results from the experiment with the conductive tape.

Table 4.3 Circuit with set up results- Conductive sheet (output voltage measurements with various materials and weight values)

	PLASTIC BAG	A4 PAPER	COTTON	POLYESTER
Without weight	3V	2V	3V	3V
1kg	2V	2V	2.5V	2.5V
2kg	2V	1.9V	2V	2.5V
5kg	2V	1.7V	2V	2.5V

Table 4.4 Circuit with set up results-Conductive tape (output voltage measurements with various materials and weight values)

	PLASTIC BAG	A4 PAPER	COTTON	POLYESTER
Without weight	1.5V	2.5V	3V	3V
1kg	1.5V	2V	2.5V	3V
2kg	1.5V	1.5V	2V	2.5V
5kg	1.5V	1.2V	2V	2.5V

It is clear again that the conductive tape seems to work better than the conductive sheet. At first, we expected the circuit to work better than the Bitalino because of the input impedance of the amplifier but we can see from the results that we have to fix the connections of the wires. For that, we insulated sensitive parts of the circuit, so that the position of the components did not affect the signal and made it noisy.

For example, we can see in a subplot the signals we took with cotton t-shirt (see Figure 4.4). We can see that the saturation is huge and the signal is not good. We can see some peaks but for sure we can't see a good and clear signal.

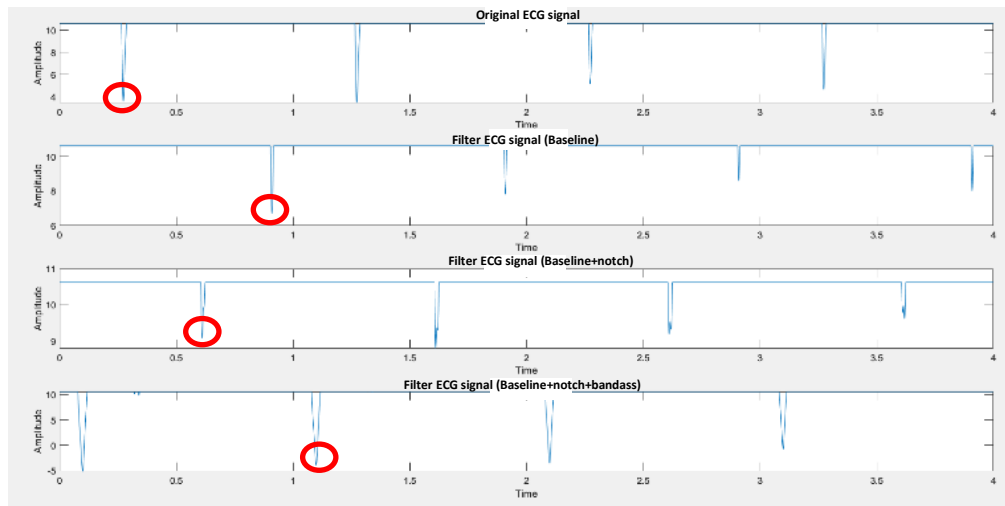


Figure 4.4 Signals of experiments with the circuit, set up and cotton t-shirt (mV/s)

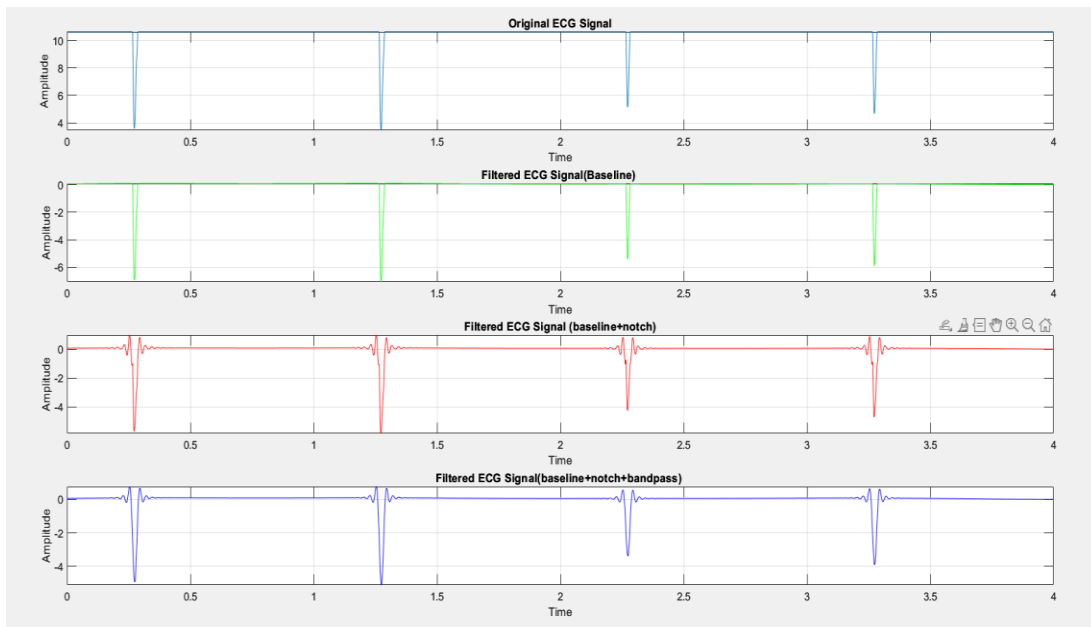


Figure 4.5 Filter signal of experiment with the circuit, set up and cotton t-shirt (mV/s)

In Figure 4.5 we can see a subplot of the filter signal using cotton t-shirt without weight. The first plot is the original cotton t-shirt without weight signal, the second plot is the same signal with a high-pass filter, the third plot is the same signal with a high-pass and a notch filter and the last one is the same filter but with a high-pass, a notch filter and a bandpass filter. We can clearly see how every filter affects the signal. The last one is a clean signal, without noise that we can detect the R-peak.

4.1.4 Results for circuit with set up and insulation

Results from the implementation CIRCUIT_SETUP_INSULATION. In the tables below we will present the results of the experiments. The amplitudes are the lowest for every case where we can observe R peaks. On table 4.5 we can see the results from the experiment with the conductive sheet and on table 4.6 we can see the results from the experiment with the conductive tape.

Table 4.5 Circuit with set up and insulation results- Conductive sheet (output voltage measurements with various materials and weight values)

	PLASTIC BAG	A4 PAPER	COTTON	POLYESTER
Without weight	50mV	50mV	220mV	250mV
1kg	25mV	25mV	200mV	200mV
2kg	20mV	20mV	150mV	150mV
5kg	20mV	15mV	100mV	150mV

Table 4.6 Circuit with set up and insulation results-Conductive tape (output voltage measurements with various materials and weight values)

	PLASTIC BAG	A4 PAPER	COTTON	POLYESTER
Without weight	50mV	50mV	50mV	50mV
1kg	20mV	20mV	40mV	40mV
2kg	15mV	15mV	30mV	30mV
5kg	15mV	10mV	20mV	20mV

It is clear that the insulation worked. We can see that the amplitudes are good and lower than Bitalino's ones. We can say that, in this environment, the circuit works better than the Bitalino. The connections now are better and the aluminum foil works as intended.

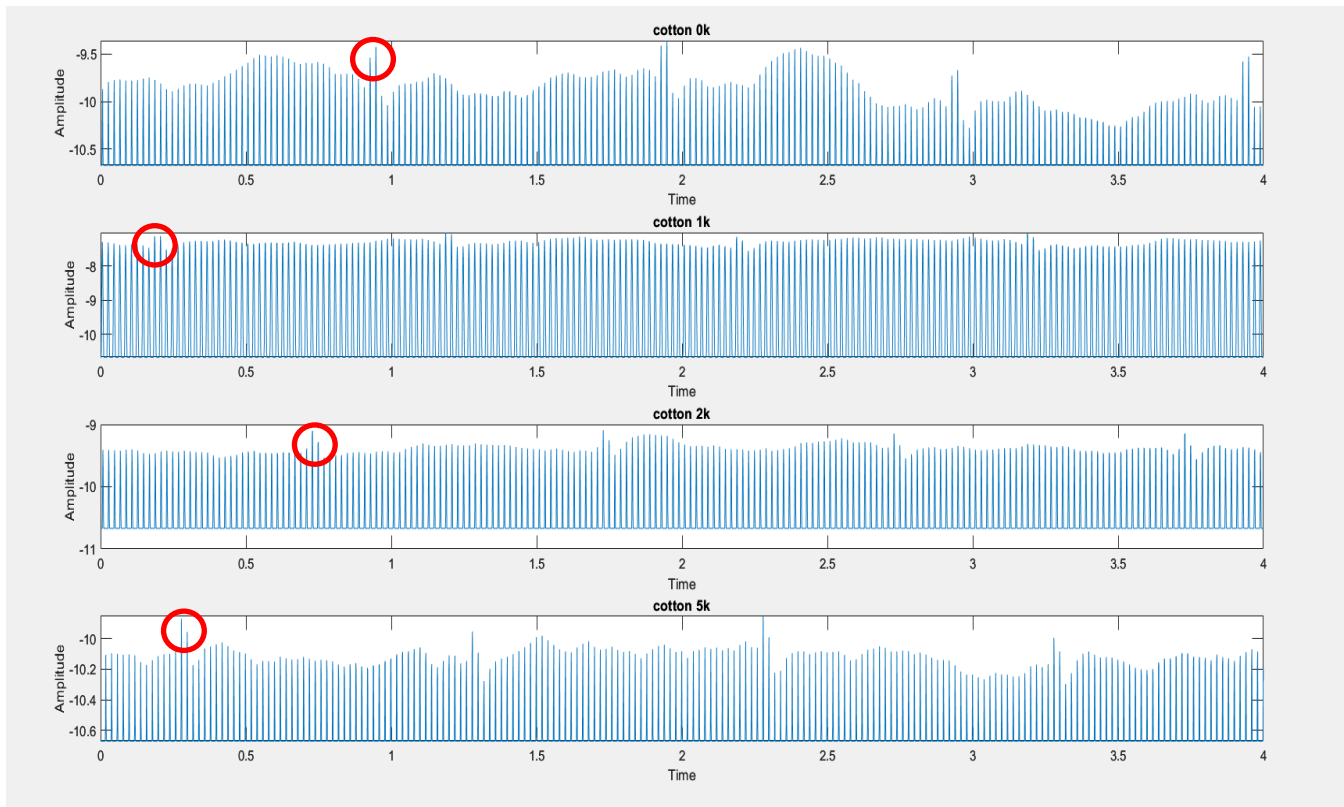


Figure 4.6 Signals of experiments with the circuit, set up, insulation and cotton t-shirt (mV/s)

In Figure 4.6 we can see a subplot of the signals using cotton t-shirt. The signal is better, and we can see R-peaks. We have a lot of noise but with a filter we can clean the signal.

In Figure 4.7 we can see a subplot of the filtered signal using cotton t-shirt without weight. The first plot is the original signal for the cotton t-shirt without weight, the second plot is the same signal with a high-pass filter, the third plot is the same signal with a high-pass and a notch filter and the last one is the same filter but with a high-pass, a notch filter and a bandpass filter. We can clearly see how every filter affects the signal. The last one is a clean signal, with less noise that we can detect the R-peaks.

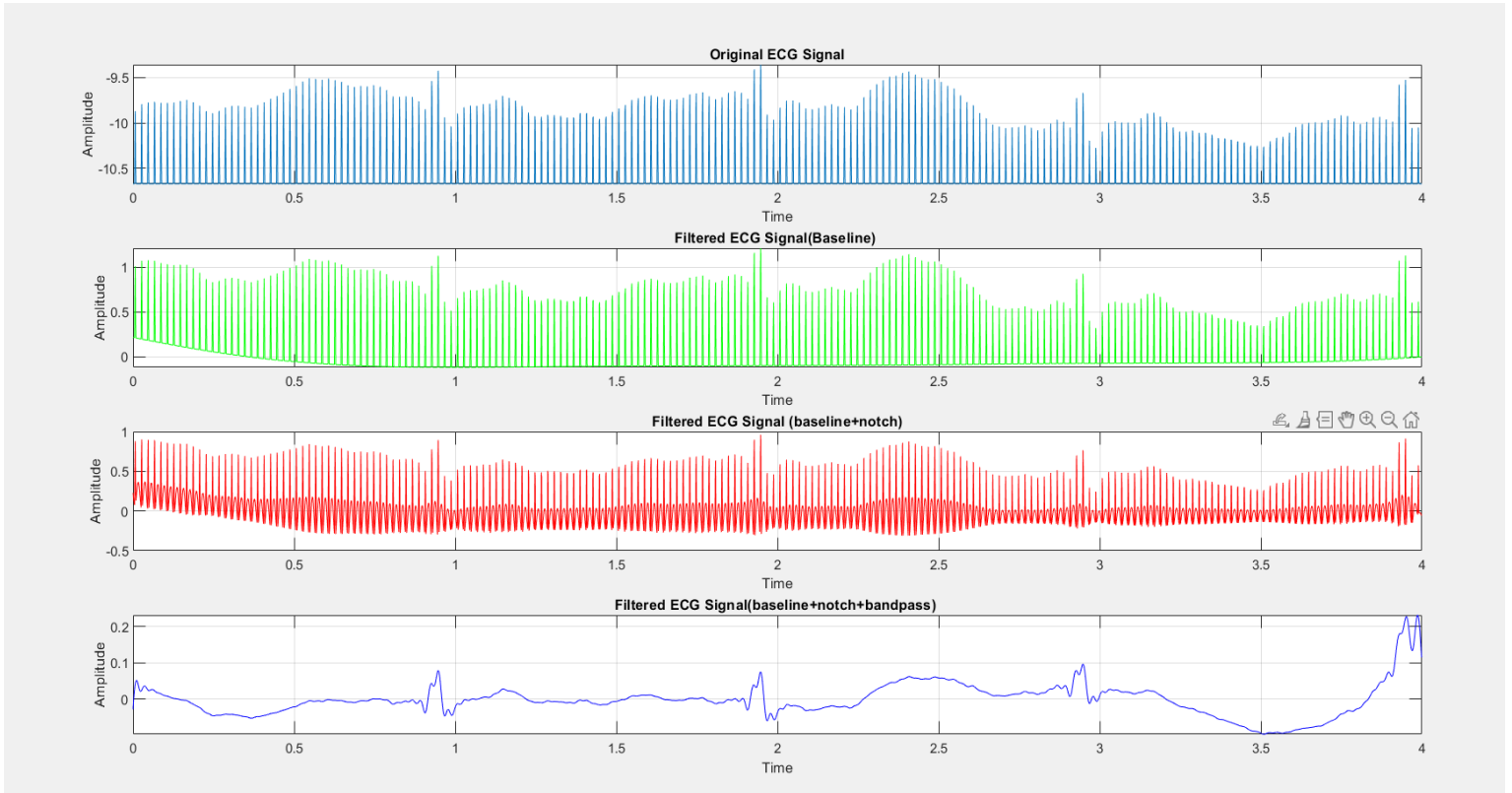


Figure 4.7 Filter signal of experiment with the circuit, set up, insulation and cotton t-shirt without weight (mV/s)

4.1.5 Result for circuit with set up, insulation and moisture

Results from the implementation CIRCUIT_SETUP_INSULATION_MOISTURE. In the tables below, we will present the results of the experiments. The amplitudes are the lowest for every case where we can observe R peaks. On the table 4.7 we can see the results from the experiment with the conductive tape.

Table 4.7 Circuit with set up, insulation and moisture results-Conductive tape (output voltage measurements with various materials and moisture values)

	PLASTIC BAG	A4 PAPER	COTTON	POLYESTER
0%	50mV	70mV	50mV	50mV
10%	50mV	50mV	5mV	5mV
20%	50mV	5mV	2mV	2mV
30%	50mV	2mV	1mV	1mV

The minimum voltages now are below those observed in other experiments. They are also closer to the ones expected from a real ECG. Our results show that the circuit should work correctly on people because of the effect of sweat. That will be tested in another experiment. In Figure 4.8 we can clearly see the R-peaks without any noise.

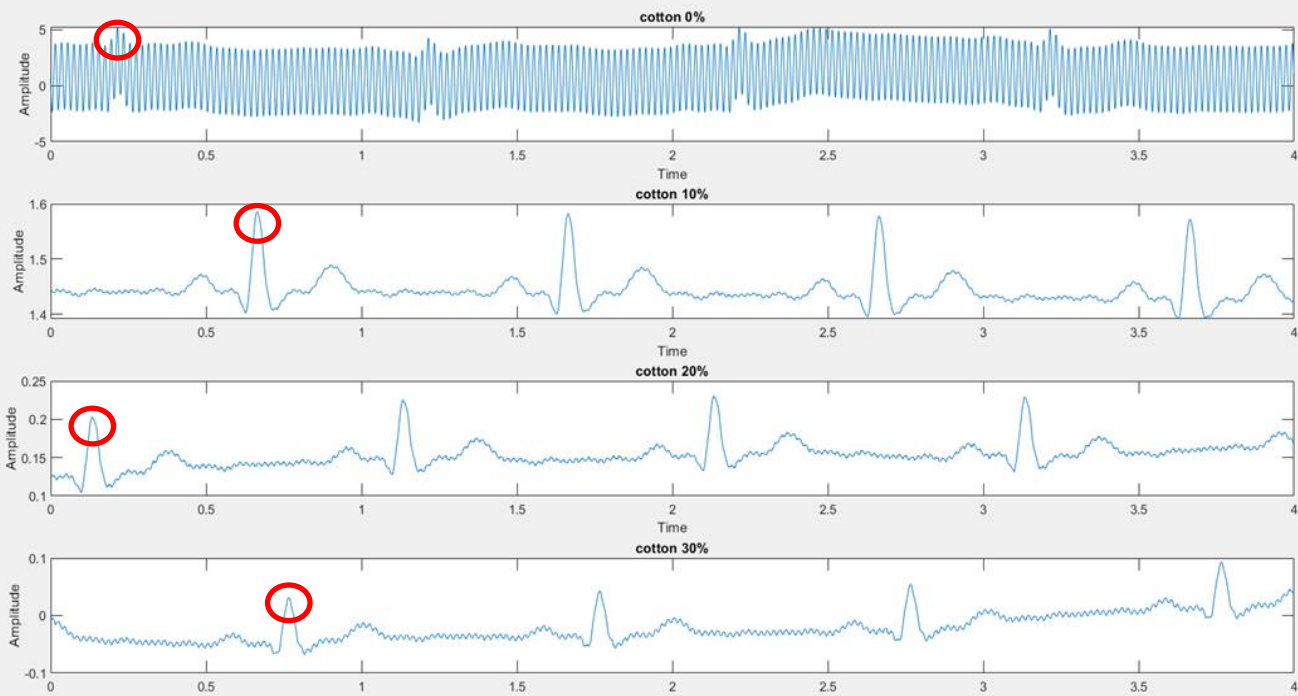


Figure 4.8 Signals of experiments with the circuit, set up, insulation, moisture and cotton t-shirt (mV/s)

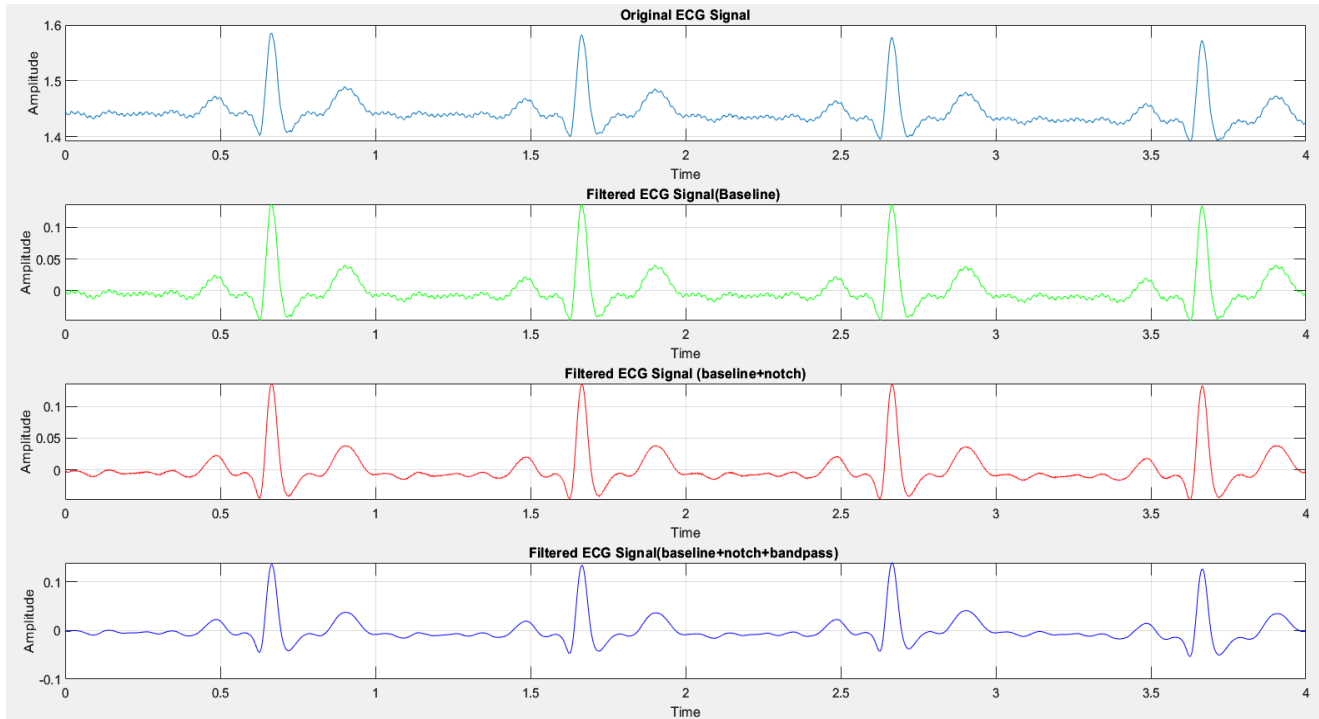


Figure 4.9 Filter signal of experiment with the circuit, set up, insulation, 10% moisture and cotton t-shirt (mV/s)

In Figure 4.9 we can see a subplot of the filter signal using cotton t-shirt without weight and with 10% moisture. The first plot is the original signal for the cotton t-shirt without weight, the second plot is the same signal with a high-pass filter, the third plot is the same signal with a high-pass and a notch filter and the last one is the same filter but with a high-pass, a notch filter and a bandpass filter. We can clearly see how every filter affects the signal. Even if the original signal is good and we can detect R-peaks, it is clear that the last one is a clean signal, without noise and we can understand better how every filter worked.

4.1.6 Bitalino with set up and moisture results

Results from the implementation BITALINO_SETUP_MOISTURE. In the tables below we will present the results of the experiments. The amplitudes are the lowest that every case can give R-peaks. On the table 4.8 we can see the results from the experiment with the conductive tape.

Table 4.8 Bitalino with insulation and moisture results-Conductive tape (output voltage measurements with various materials and moisture values)

	PLASTIC BAG	A4 PAPER	COTTON	POLYESTER
0%	4V	5V	5V	5V
10%	4V	5mV	5mV	10mV
20%	4V	2mV	2mV	5mV
30%	4V	1mV	1mV	2mV

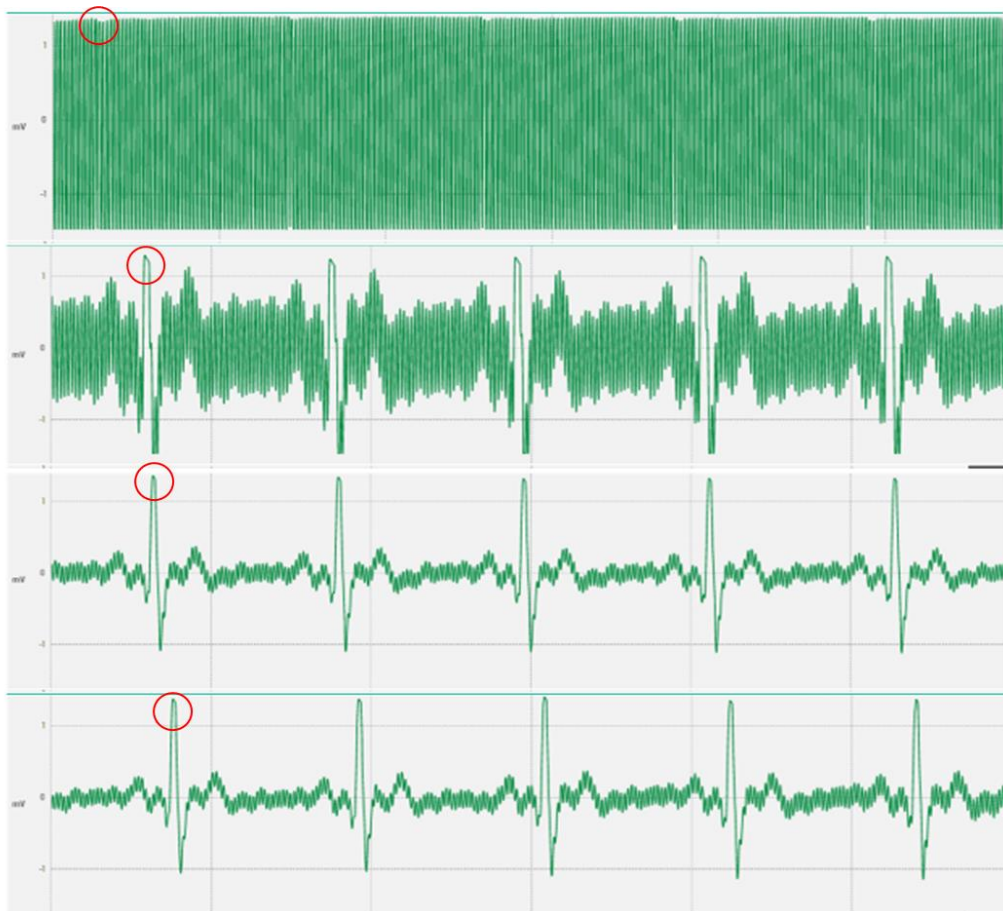


Figure 4.10 Signals of experiments with the Bitalino, set up, moisture and cotton t-shirt (0,10,20,30%) (mV/s)

It is clear that Bitalino works better with moisture as the difference between the voltage without moisture is of 3 orders of magnitude. We can see that the moisture changes the way that the Bitalino works with non-contact. So, when someone sweats the system should work properly. In Figure 4.10 we can see a subplot of the signals using cotton t-shirt. The signal is clearer, as more features of the ECG wave can be distinguished.

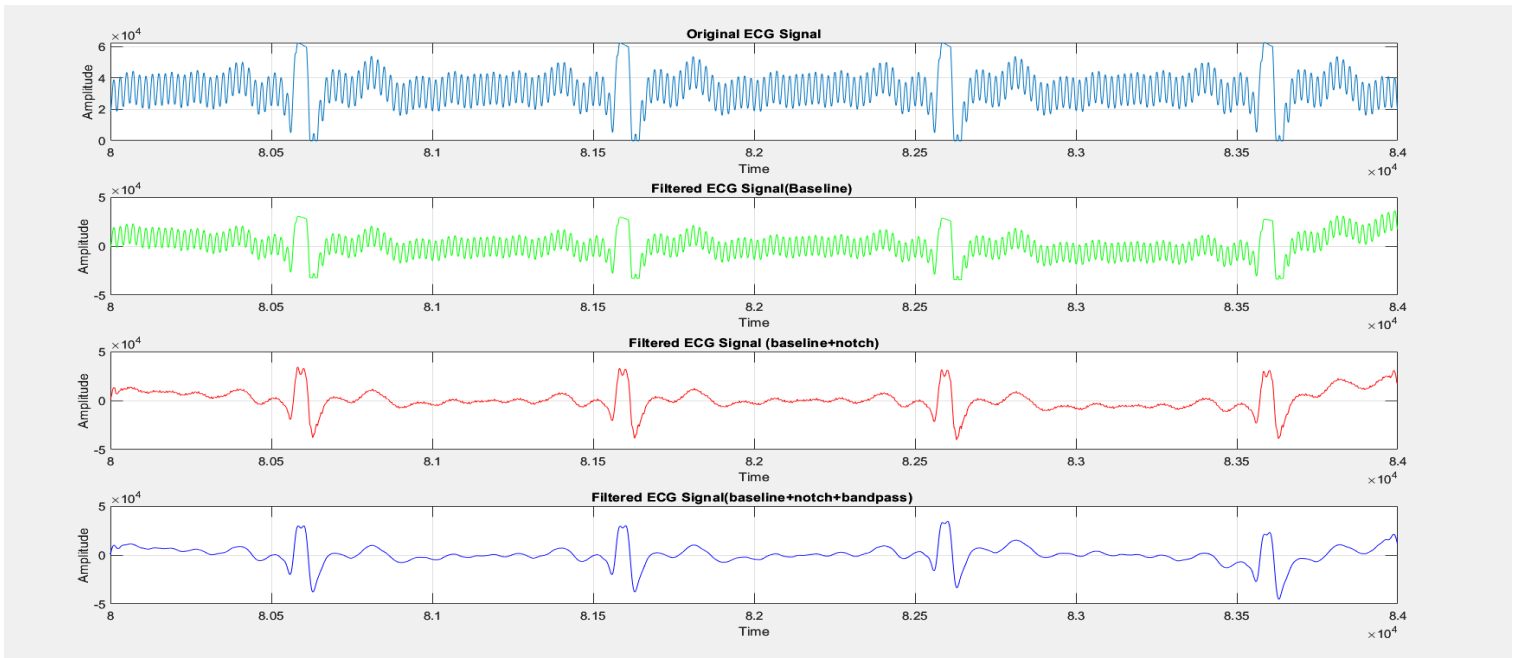


Figure 4.11 Filter signal of experiments with the Bitalino, set up, 10% moisture and cotton t-shirt (mV/s)

In Figure 4.11 we can see a subplot of the filter signal using cotton t-shirt without weight and with 10% moisture. The first plot is the original cotton t-shirt without weight signal, the second plot is the same signal with a high-pass filter, the third plot is the same signal with a high-pass and a notch filter and the last one is the same filter but with a high-pass, a notch filter and a bandpass filter. We can clearly see how every filter affects the signal. The original signal is a bit noisy but we can detect R-peaks. It is clear that the last one is a clean signal, without noise and we can understand better how every filter worked.

We can see that the x and y axis are not correct. This happened because the file with the signal from Bitalino is has samples and no seconds. For that, the time axis is 80.000, which means the 1.3th minute of the recordings ($80.000/1000=80$, $80/60=1.3$ minute). So, in this Figure we can see the first 4 seconds from the 1.3th minute. This Figure is showing the ADC conversion values without having been translated back to physical units. The data was represented as a 16-bit integer, hence the scale value.

4.1.7 Results for circuit with set up, insulation and small electrodes

Results from the implementation CIRCUIT_SETUP_INSULATION_2cm_ELECTRODES. In the tables below, we will present the results of the experiments. The amplitudes are the lowest that every case can give R-peaks. On the table 4.9 we can see the results from the experiment with the conductive tape.

Table 4.9 Circuit with set up, insulation results and small electrodes (output voltage measurements with various materials and weight values)

	PLASTIC BAG	A4 PAPER	COTTON	POLYESTER
Without weight	70mV	50mV	50mV	50mV
1kg	50mV	40mV	40mV	40mV
2kg	40mV	30mV	30mV	30mV
5kg	30mV	20mV	20mV	20mV

Compared to the table 4.6 we can see that for the plastic and the paper the small electrodes need more amplitude to give signal, but for cotton and polyester there are exactly the same amplitudes. In Figure 4.12 we can see that the signal is very noisy.

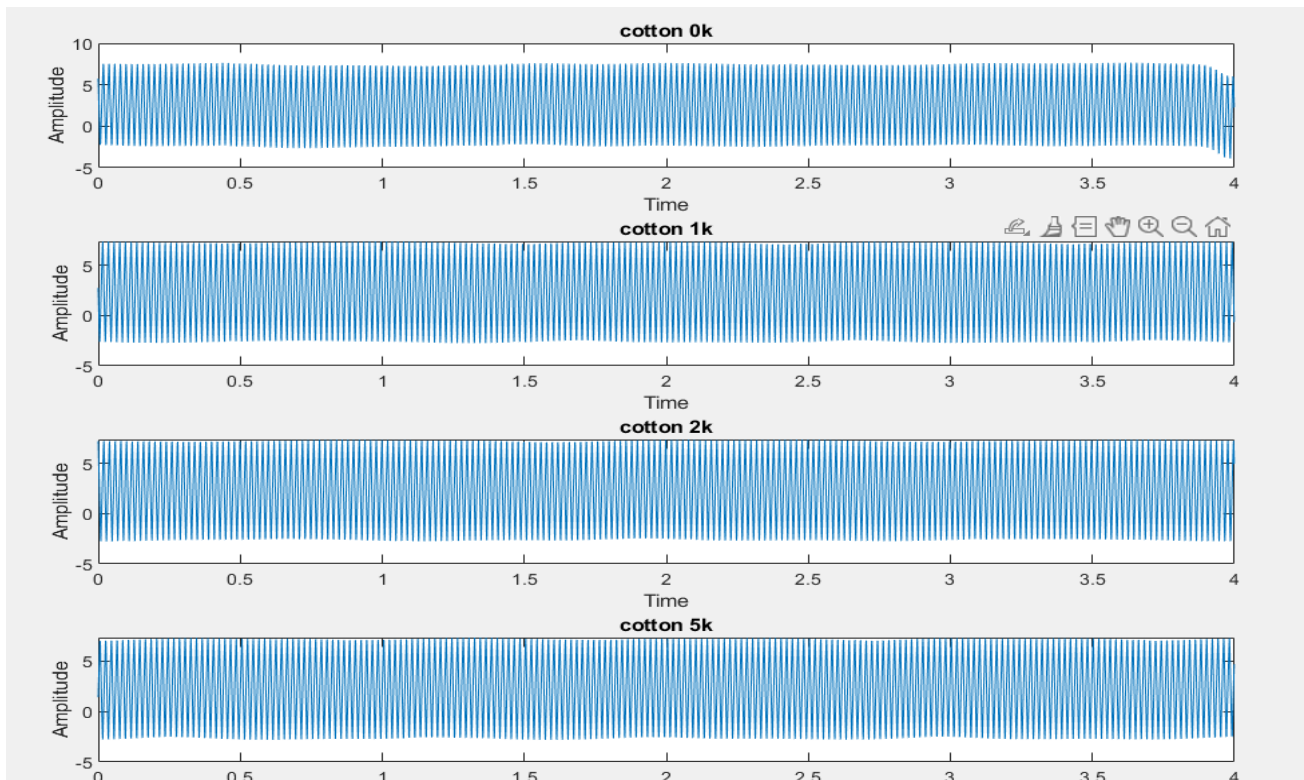


Figure 4.12 Signal of experiment with the circuit, set up, insulation, small electrodes and cotton t-shirt (mV/s)

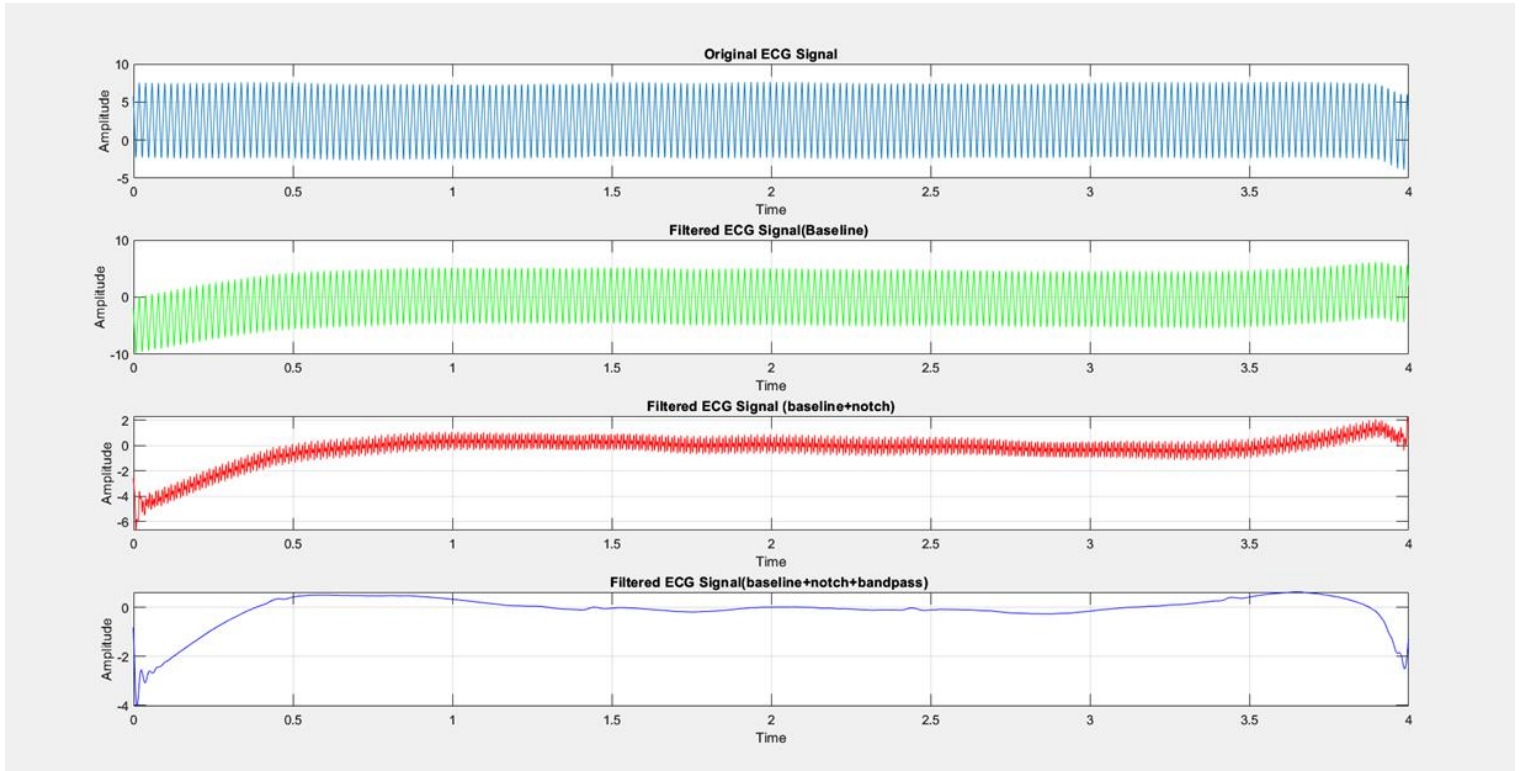


Figure 4.13 Filter signal of experiment with the circuit, set up, insulation, small electrodes and cotton t-shirt without weight (mV/s)

In Figure 4.13 we can see a subplot of the filter signal using cotton t-shirt without weight. The first plot is the original cotton t-shirt without weight signal, the second plot is the same signal with a high-pass filter, the third plot is the same signal with a high-pass and a notch filter and the last one is the same filter but with a high-pass, a notch filter and a bandpass filter.

We can clearly see how every filter affects the signal. The last one is a clean signal, with less noise that we can detect the R-peaks.

So, we can say that the small electrodes give more noise to our signal and it is not very easy to detect R-peaks.

4.1.8 Results for circuit2 with set up, insulation and reference

Results from the implementation CIRCUI2_SETUP_INSULATION_REFERENCE. In the tables below, we will present the results of the experiments. The amplitudes are the lowest that every case can give R-peaks. On the table 4.10 we can see the results from the experiment with the conductive tape.

Table 4.10 Circuit2 with set up, insulation and reference (output voltage measurements with various materials and weight values)

	COTTON	POLYESTER
Without weight	30mV	30mV
1kg	20mV	20mV
2kg	10mV	15mV
5kg	7mV	10mV

Compared to the table 4.6 we can see that with the circuit2 (circuit1 with reference and extra components for the input signal) we can detect R-peaks in lower amplitudes. That means that the signal now is less noisy and more stable. In Figure 4.14 we can see a subplot of the signals using cotton t-shirt.

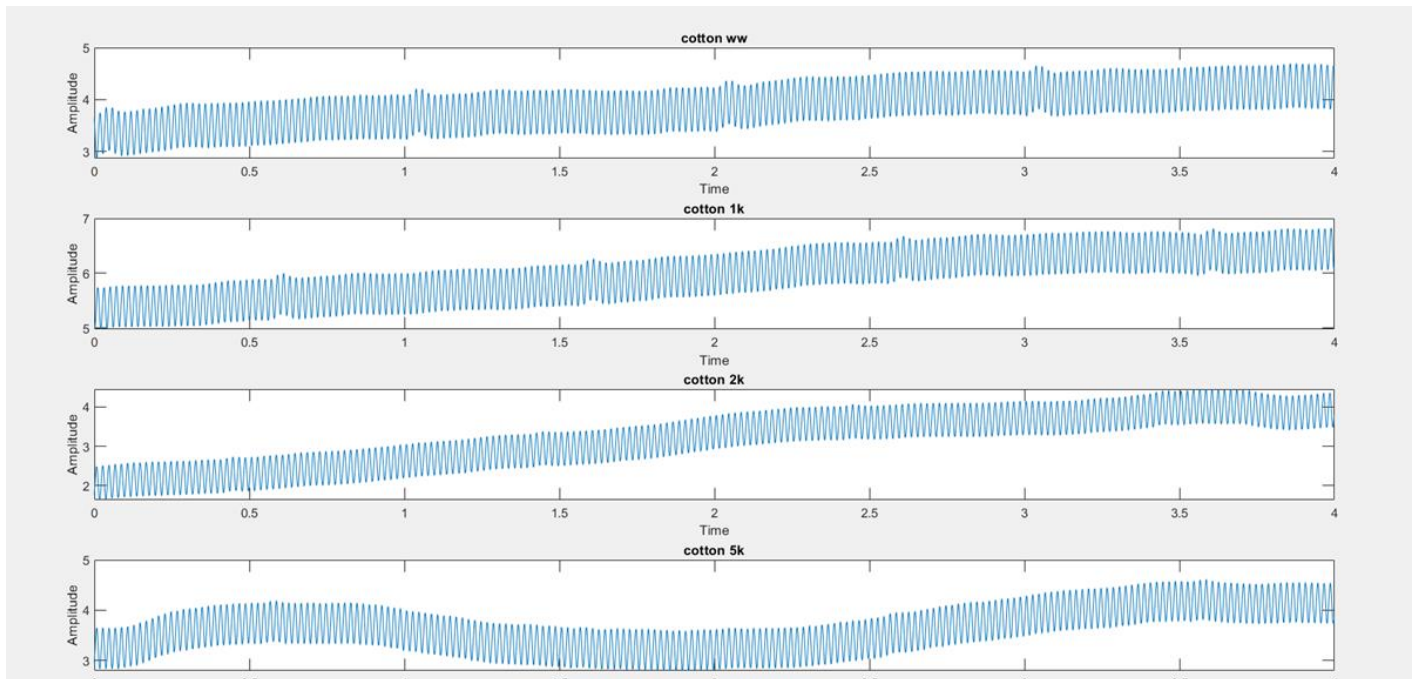


Figure 4.14 Filter signal of experiment with the circuit2, set up, insulation, reference and cotton t-shirt (mV/s)

In Figure 4.15 we can see a subplot of the same experiment with circuit1 and circuit2. It is clear that the circuit2 gives signal with less amplitude and it doesn't have saturation. Moreover, it looks more stable and closer to a real ECG signal.

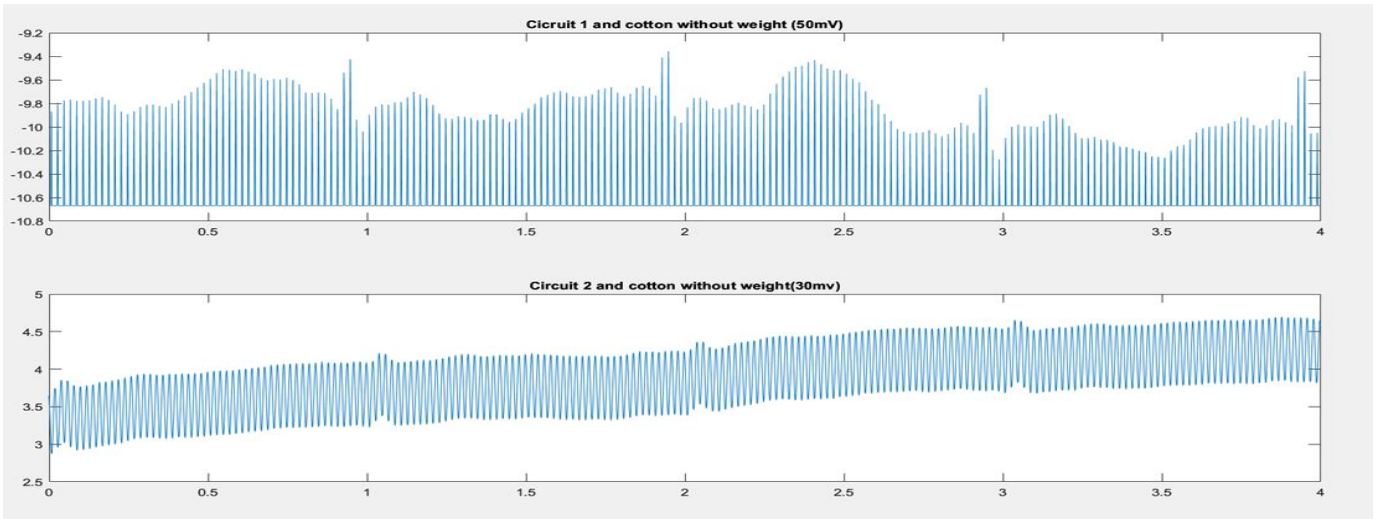


Figure 4.15 Circuit1 vs circuit2 (mV/s)

In Figure 4.16 it is the filter signal with cotton t-shirt and 5 kilograms. The last signal does not have noise and we can easily detect the R-peaks.

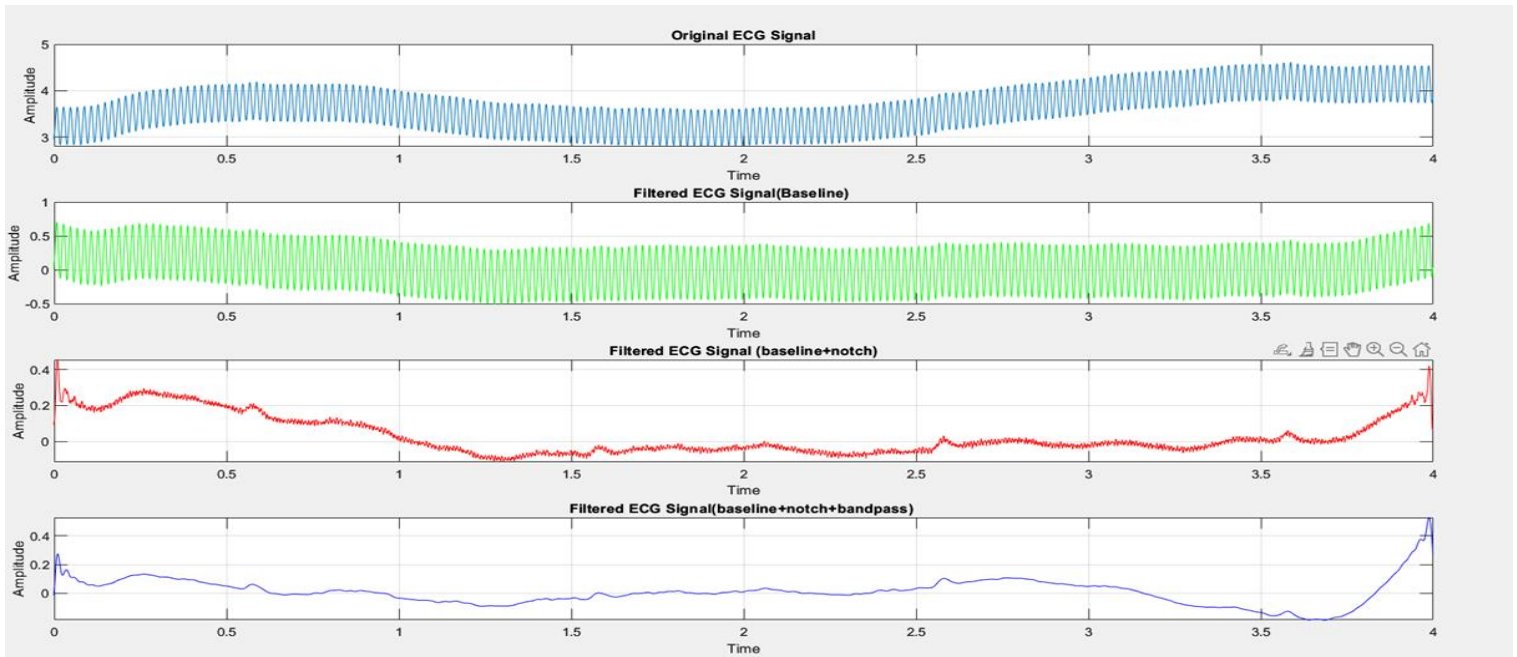


Figure 4.16 Filter signal of experiment with the circuit2, set up, insulation, reference and cotton t-shirt with 5 kilograms (mV/s)

4.2 Results for the experiments with volunteers

4.2.1 Results for the 30 minutes experiment

Results from the implementation CIRCUI2_30_MINUTES. In Figure 4.17 and in Figure 4.18 we can see 5 seconds of the signal that we took from the 30 minutes experiment. In Figure 4.16 the first 5 seconds of the 3rd minute, and we can see that the signal is not good. We can detect 3 R-peaks on the filtered signal, but the quality is not good. On the second is the first 5 second of the 28th minute. We can detect 7 peaks on both raw and filtered signal and the signal is not very noisy.

So, we confirm the fact that as time passes and the person sweats more, the peaks become clearer and less noisy. Even if the signal is not perfect, it seems that the prototype circuit that we made works as it should.

In the Appendix 2 you can see in detail the evolution of the signal from 3rd to 28th minute and how the baseline wander change.

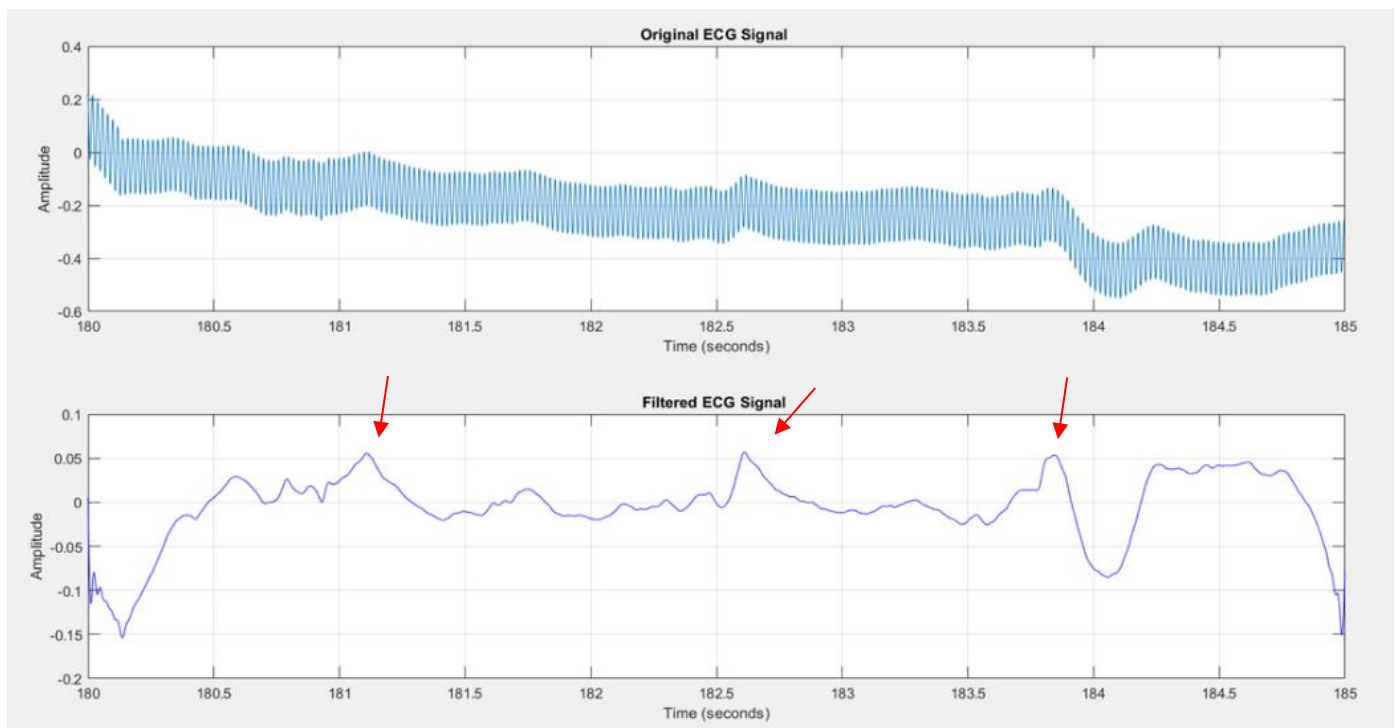


Figure 4.17 3rd minute of the 30th minutes experiment (mV/s)

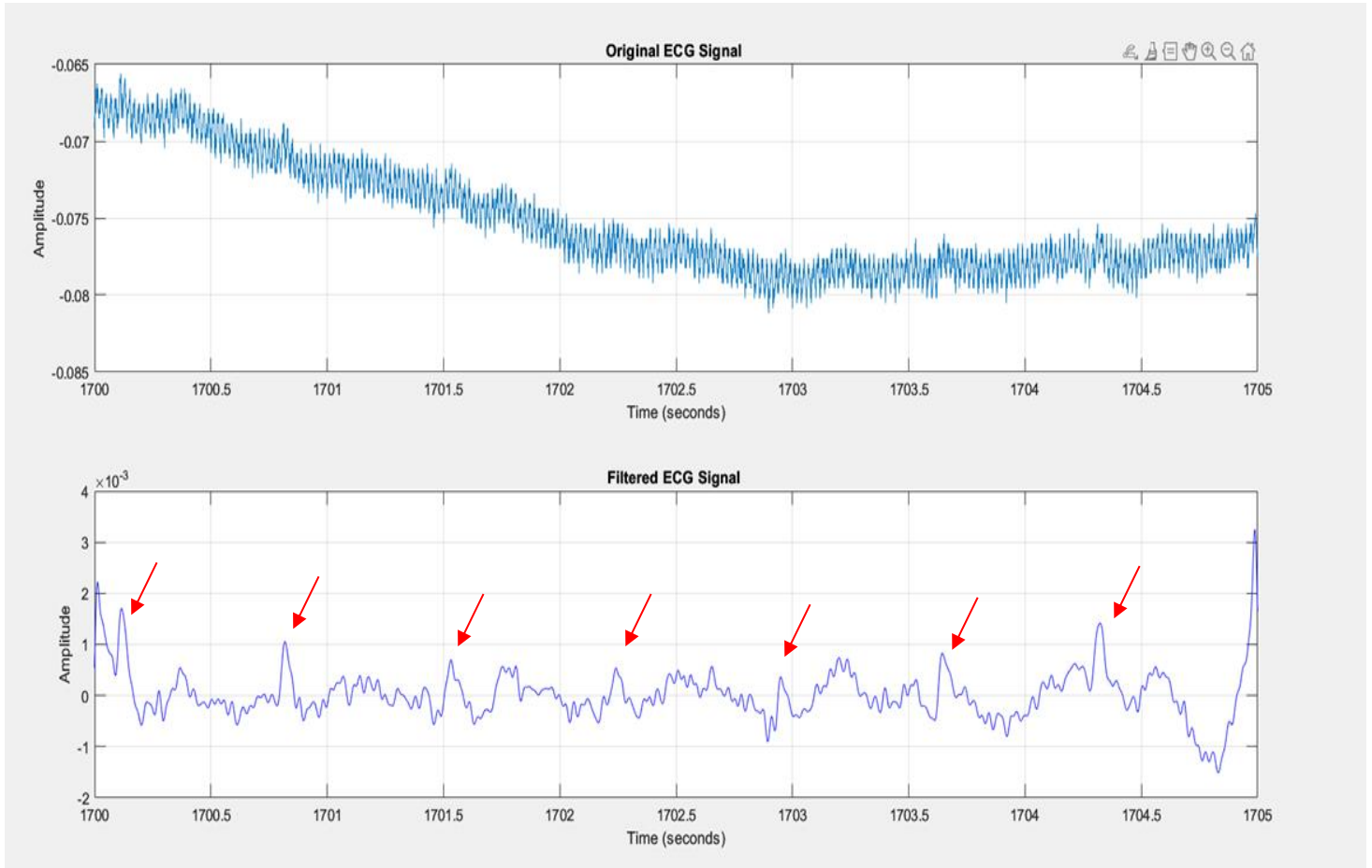


Figure 4.18 28th minute of the 30th minutes experiment (mV/s)

4.2.2 Results for the volunteers experiment with moisture

Results from the implementation CIRCUIT2_VOLUNTEERS_MOISTURE. In the Figure 4.19 we can see a subplot of the signals of subject 5. In the experiment without moisture, it is very easy to detect R-peaks.

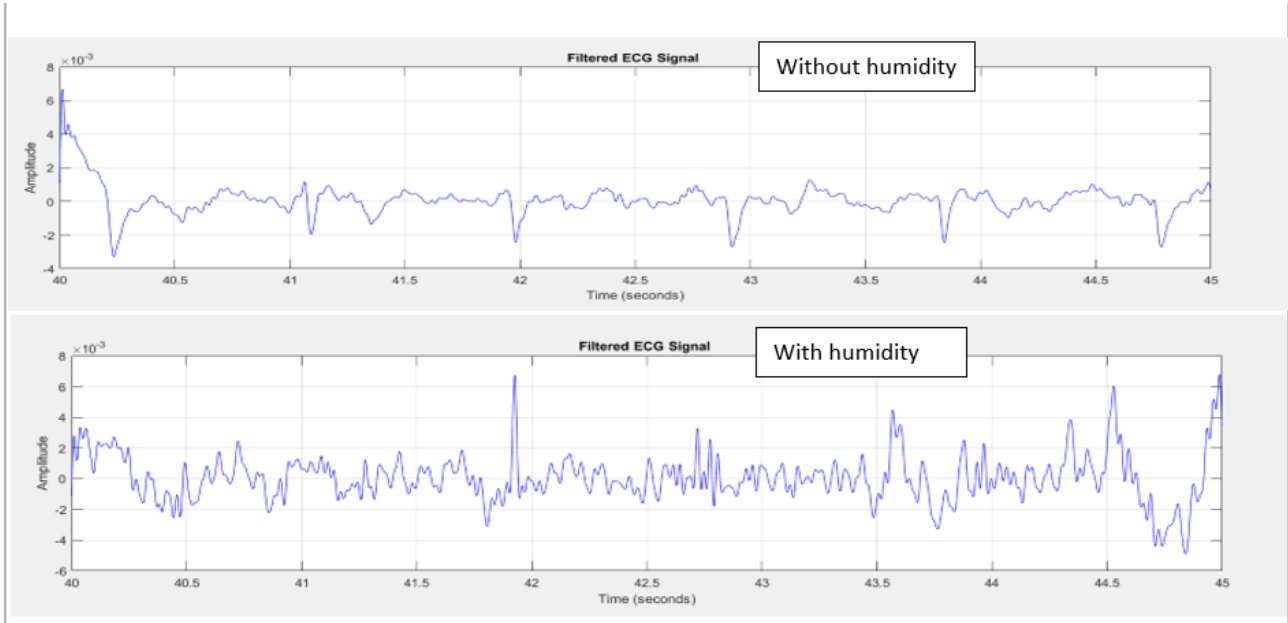


Figure 4.19 Filter signal of subject 5, without and with moisture (mV/s)

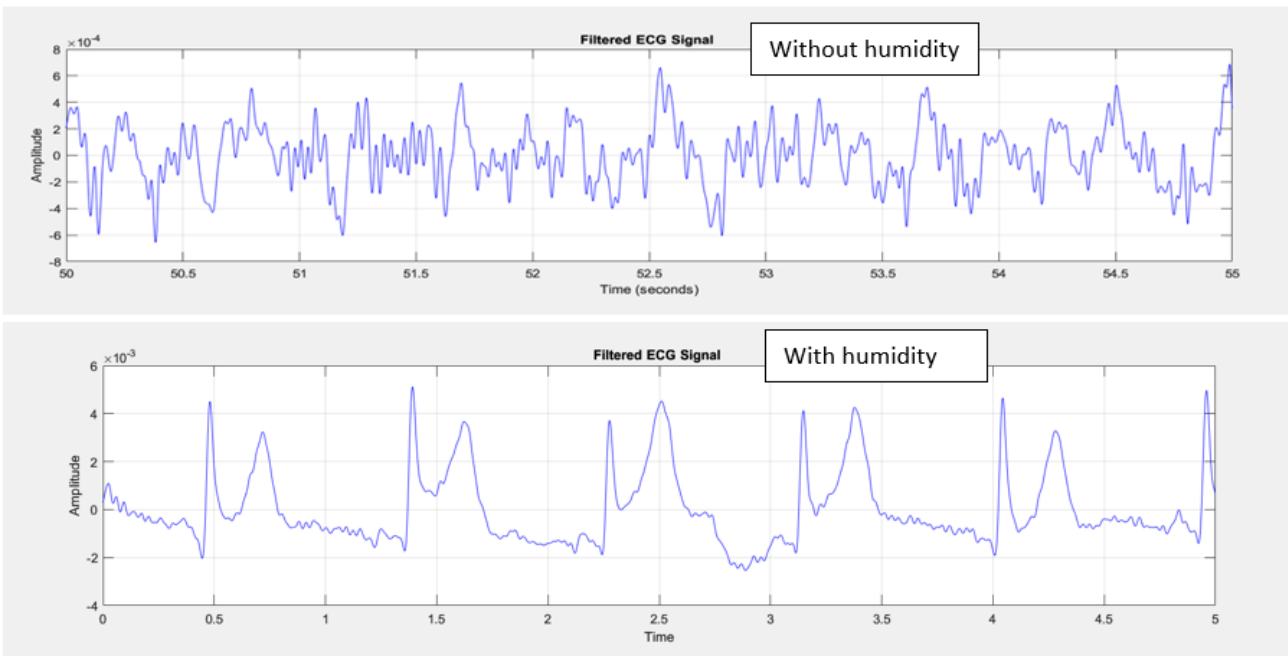


Figure 4.20 Filter signal of subject 6, without and with moisture (mV/s)

In the Figure 4.20 we can see a subplot of the signal of subject 6. In the experiment with moisture, it is very easy to detect R-peaks and the signal is almost perfect but without moisture the signal is very noisy.

It is evident that detecting R-peaks varied among subjects, with some showing better detection without moisture and others with moisture. While we could identify some peaks in both experiments, the trials conducted under moisture yielded better overall results. Therefore, our hypothesis about the impact of moisture is indeed supported.

On the table 4.11 we can see the results from the mSQI method. In both experiments, the algorithm successfully detected ECG peaks. For 6 out of the 8 participants, the mean values were better in the moisture experiments, while only 2 out of the 8 had better means in the non-moisture experiments. This indicates that our prototype system performed better under humid conditions for 75% of the volunteers.

Table 4.11 Results from mSQI method (mean and standard deviation of detection of ECG peaks)

	Without moisture	Moisture
Subject 1	Mean=0.187978 SD=0.119816	Mean=0.380654 SD=0.186293
Subject 2	Mean=0.521492 SD=0.103380	Mean=0.248582 SD=0.136427
Subject 3	Mean=0.108267 SD=0.076453	Mean=0.267250 SD=0.200523
Subject 4	Mean=0.137539 SD=0.089373	Mean=0.224433 SD=0.140954
Subject 5	Mean=0.322433 SD=0.206343	Mean=0.176840 SD=0.085656
Subject 6	Mean=0.092343 SD=0.057627	Mean=0.316931 SD=0.149283
Subject 7	Mean=0.240594 SD=0.169559	Mean=0.290018 SD=0.152900
Subject 8	Mean=0.146947 SD=0.089905	Mean=0.389795 SD=0.110154

In the Figure 4.21 a bar plot was employed to visually represent the mean values of experiments with and without moisture.

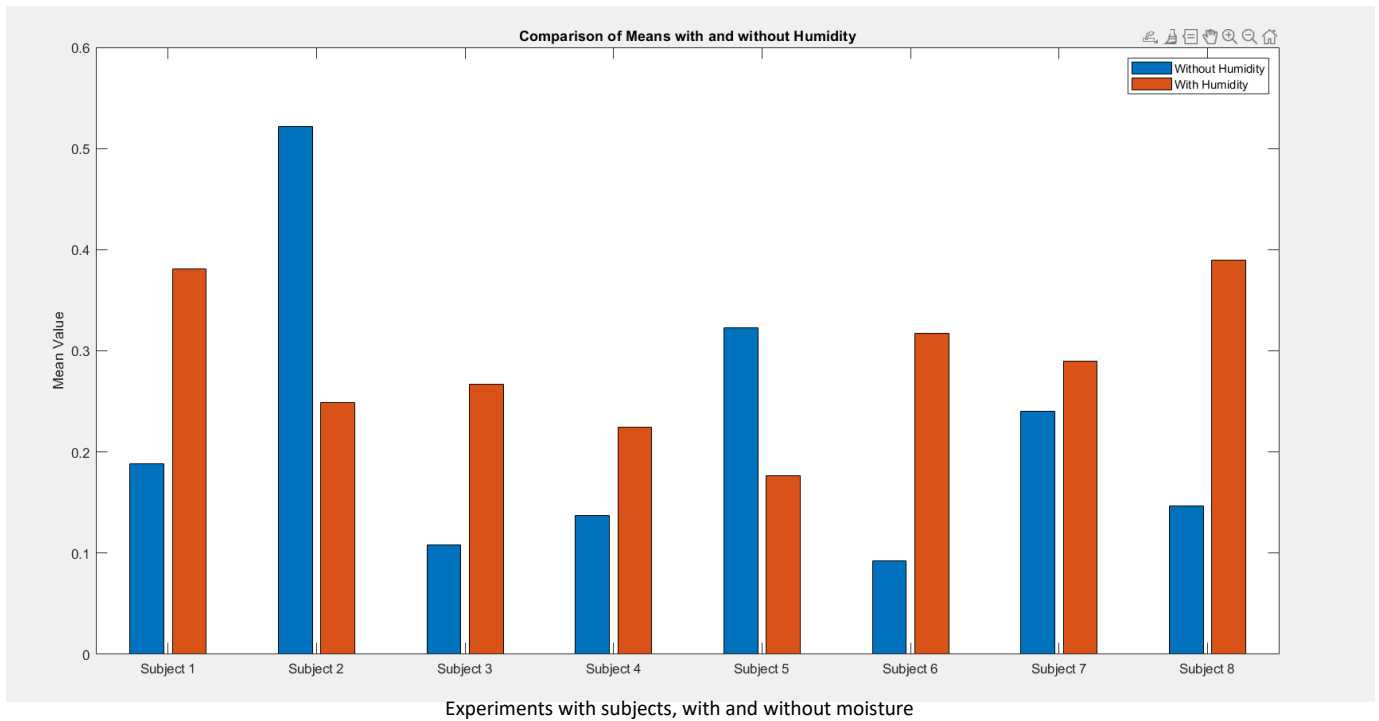


Figure 4.21 Comparison of means with and without moisture

5. Discussion and Conclusions

The final goal of this study is to build a cECG sensor that could be integrated into furniture. We started by making a first circuit with a Sallen-Key filter for the calibration experiments. We decided to characterize materials and conditions. At first, we tested two different materials for the electrodes (conductive nylon fabric tape and silver-plated nylon sheet). Several materials were tested between the electrode and a simulation of the heartbeat made with the wave generator (plastic, paper, cotton and polyester). All the tests with the conductive tape worked better. Regarding the material between the electrode and the source of the heartbeat, clearly the plastic was worse, while there is not much difference between the others (see Tables 4.3 and 4.4). In these tests a commercial sensor (Bitalino) was compared with the sensor made in the project. On the test bench the signal was always clearer with our sensor (see Tables 4.1, 4.2, 4.3 and 4.4).

After that we put insulation to the circuit and the wires to reduce the noise. It was enough to bring a signal in the range of 10-250 mV, depending on the material, to acquire the signal (see tables 4.5 and 4.6). In this case again the results with the conductive tape were better. That is why we decided to continue the experiments only with the tape.

We did tests in which a little moisture was added to the electrode, which according to the literature has an important role in the non-contact ECG. When moisture was added to the test bench with cotton and polyester, it became possible to acquire the signal when it had an amplitude of only 1 mV. That increasing from 0% to 10% humidity reduced the amplitude of the source signal from 50 to 5 mV to be able to be acquired. All materials showed a reduction except for plastic, probably because it is completely impermeable and does not create a resistive path between the electrode and the wave generator (see Table 4.7). When the sensor was compared again with the Bitalino (see Table 4.8), the amplitude of the signals was generally higher in order to register the signal. After this, no more experiments with the Bitalino were made.

Furthermore, the size of the electrodes was tested to be reduced to 2 cm², requiring a higher amplitude in the signal to be able to register it (see Table 4.9). We saw that the amplitude was almost the same but the final signal had noise, and for that we decided to return to the original size of the electrodes.

For the volunteers tests we created a new circuit with a reference electrode. When the reference was added, the signal became less noisy and it was possible to detect signals with a lower amplitude (see Table 4.10). We built a new set up with a chair and a layer of foam and we made two different tests. First a 30 minutes test to see how the time will react the quality of the signal. In Figures 4.16 and 4.17 we can see that the waves corresponding to the heartbeats could be seen and it was observed that over time they were clearer. Then we tested 8 volunteers for 1 minute each for an experiment with and without moisture. In 6 of the cases the heartbeats were clearer when moisture has been used, although in two cases not.

We used MatLab code to filter all the signals with a High-Pass Filter, a notch filter and a bandpass filter. At the end we used the mSQI algorithm to find the means of the signals and to compare these signals, obtaining a higher value in 6 of the 8 subjects (see Table 4.11).

We have to say that the quality of the signal is not ideal. This happens because we tested a prototype system that we made with a few components and the environmental conditions that the experiments took place were not the best possible, because we were into a lab with a lot of people and other machines that produced noise to our system.

About the Bitalino experiments, it is clear that it is not an ideal equipment for non-contact ECG. Compared to our circuits it seems that our circuit works better. Both worked better with the addition of moisture.

During the experiments we tried several ideas that we saw in the literature. One of them is the addition of a resistor and a capacitor to the input before the electrodes [20]. We can say that this helped us a lot and increased the quality of our signal. From the other hand, we already mentioned how the moisture can change completely the quality of the signal. We found in a lot of papers [14] that if you add a thin layer of medical gel between the capacitive electrodes and the human body this can help the signal. In our case, this didn't help, and the result was a saturation signal. Moreover, we tried to improve the reference electrode with adding a passive reference circuit with an amplifier and some components. This also didn't work for our case and we didn't have the time to make changes for it to work.

Future steps could focus on embedding the sensor directly into beds and refining circuit design and insulation for improved performance and practicality. This research establishes a foundational framework for advancing non-invasive ECG monitoring technology, promising significant applications in healthcare and beyond.

References

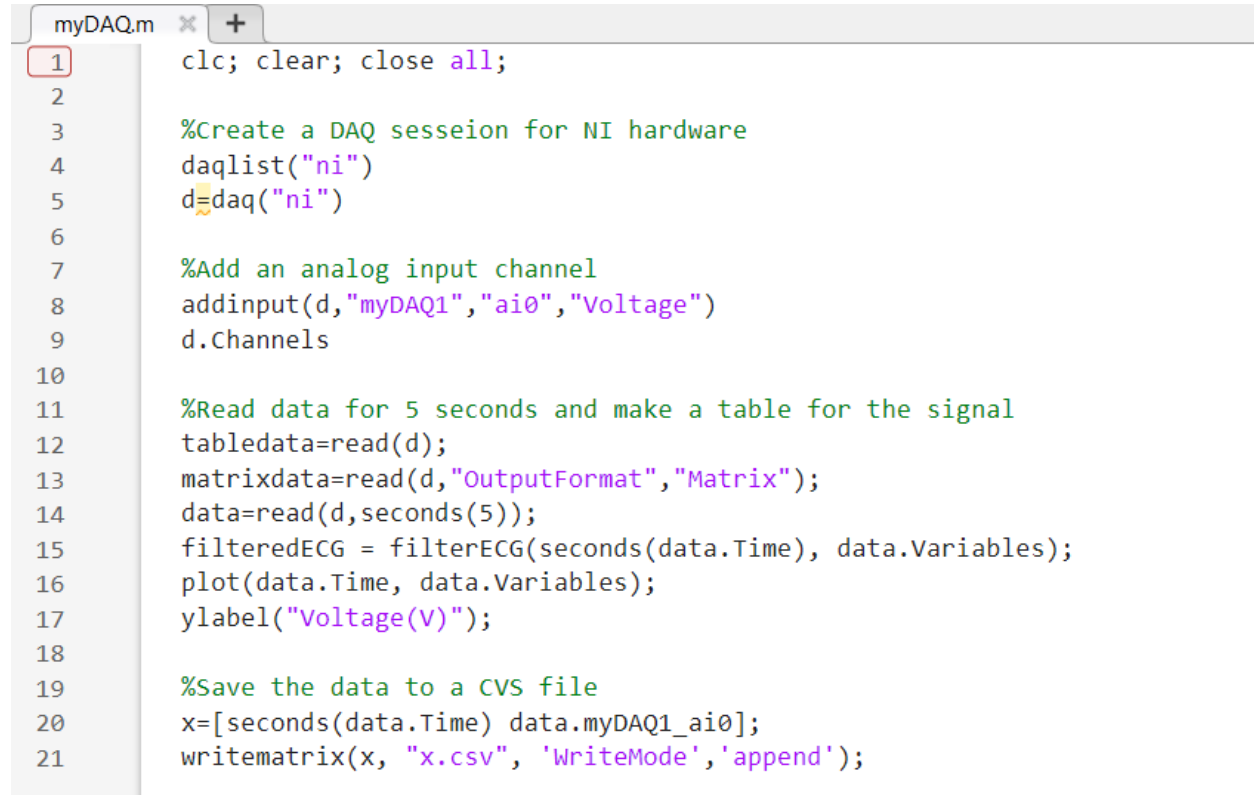
- [1] Selcan, K.B., Uysal, A.K. & Gunal, E.S., 2018. A survey on ECG analysis. *Biomedical Signal Processing and Control*, pp. 216-235. Available at: <https://www.sciencedirect.com/science/article/abs/pii/S1746809418300636>.
- [2] Xiao, Z., Xing, Y., Yang, C., Li, J. & Liu, C., 2022. Non-Contact Electrocardiograms Acquisition Method Based on Capacitive Coupling. *IEEE Instrumentation & Measurement Magazine*, pp. 53-61. Available at: https://www.researchgate.net/publication/359910273_Non-Contact_Electrocardiograms_Acquisition_Method_Based_on_Capacitive_Coupling.
- [3] Takano, M. & Ueno, A., 2019. Noncontact In-Bed Measurements of Physiological and Behavioral Signals Using an Integrated Fabric-Sheet Sensing Scheme. *IEEE Journal of Biomedical and Health Informatics*. Available at: <https://ieeexplore.ieee.org/stamp/stamp.jsp?arnumber=8355475>.
- [4] Jacqueline, G.M. & Anthony, C.J., 2010. *12-Lead EKG Confidence: A step-by-step guide*. Springer Publishing Company. ISBN: 978-0826118127.
- [5] Anaesthasier,2023, "The Cardiac Action Potential," , Available at: <https://www.anaesthasier.com/the-cardiac-action-potential/>.
- [6] Fogoros, R.N., 2012. *Electrophysiologic Testing*. WILEY-BLACKWELL. ISBN: 978-1118620949.
- [7] Studentdoctor, 2019, "The Cardiac Action Potential," Available at: <https://www.studentdoctor.net>.
- [8] "nataliescasebook," 2019. [Online]. Available: <http://www.nataliescasebook.com/tag/e-c-g-basics>.
- [9] Gargiulo, G.D., Bifulco, P., Cesarelli, M., McEwan, A.L., Moeinzadeh, H., O'Loughlin, A., Shugman, I.M., Tapson, J.C. & Thiagalingam, R., 2018. On the Einthoven Triangle: A Critical Analysis of the Single Rotating Dipole Hypothesis. *Sensors*. Available at: [ResearchGate](https://www.researchgate.net/publication/324111111).
- [10] Hampton, J., 2019. *The ECG Made Easy*. ELSEVIER. ISBN: 978-0702074578. Available at: <https://www.elsevier.com/books/the-ecg-made-easy/hampton/978-0-7020-7457-8>.
- [11] Chow, H.C. & Jia-Yu, W., 2007. High CMRR instrumentation amplifier for biomedical applications. *IEEE*. Available at: <https://ieeexplore.ieee.org/abstract/document/4555532>.

- [12] Xu, P.J., Zhang, H. & Tao, X.M., 2008. Textile-structured electrodes for electrocardiogram. *Taylor and Francis*, pp. 183-213. Available at: <https://www.tandfonline.com/doi/abs/10.1080/00405160802597479>.
- [13] Li, X. & Sun, Y., 2017. NCMB-Button: A Wearable Non-contact System for Long-Term Multiple Biopotential Monitoring. *IEEE*. Available at: <https://ieeexplore.ieee.org/document/7950971>.
- [14] Sibrecht, B., Wei, C., Feijs, L. & Oetomo, S.B., 2009. Smart Jacket Design for Neonatal Monitoring with Wearable Sensors. *IEEE*. Available at: <https://ieeexplore.ieee.org/abstract/document/5226899>.
- [15] akano, M. & Ueno, A., 2019. Noncontact In-Bed Measurements of Physiological and Behavioral Signals Using an Integrated Fabric-Sheet Sensing Scheme. *IEEE Journal of Biomedical and Health Informatics*. Available at: <https://ieeexplore.ieee.org/abstract/document/8355475>.
- [16] Ortega, M.B., 2023. Design and development of a capacitive ECG sensor. Degree thesis, Universidad San Pablo-CEU. (unpublished).
- [17] Adafruit, Conductive Nylon Fabric Tape. Available at: <https://www.adafruit.com/product/3960#technical-details>.
- [18] Kitronik, Silver-plated nylon. Available at: <https://kitronik.co.uk/products/2716-conductive-fabric-ripstop>.
- [19] Texas Instruments, 2022. INA12x Precision, Low-Power Instrumentation Amplifiers. Available at: <https://www.ti.com/lit/ds/symlink/ina128.pdf>.
- [20] Yang, H. et al., 2024. Paper-based microfluidic chip for. *Sensors and Actuators: A. Physical*. Available at: <https://www.sciencedirect.com/science/article/abs/pii/S0924424724002577>.
- [21] Parente, F.R., Santonico, M., Zompanti, A., Benassai, M., Ferri, G., D'Amico, A. & Pennazza, G., 2017. An Electronic System for the Contactless Reading of ECG Signals. *Sensors*. Available at: <https://www.mdpi.com/1424-8220/17/11/2474>.
- [22] Zhao, Z. & Zhang, Y., 2018. SQI Quality Evaluation Mechanism of Single-Lead ECG Signal Based on Simple Heuristic Fusion and Fuzzy Comprehensive Evaluation. *Frontiers in Physiology*, 9, p.727. Available at: <https://www.frontiersin.org/journals/physiology/articles/10.3389/fphys.2018.00727/full>.
- [23] A. Grech, C. García and P. Perez-Tirador, 2023, "A metric index to assess the quality of wearable ECG recordings," in *A. IEEE 19th International Conference on Body Sensor Networks*, Boston.

- [24] Navaz, A.N., Mohammed, E., Serhani, M.A. & Zaki, N., 2016. The use of data mining techniques to predict mortality and length of stay in an ICU. *IEEE*. Available at: <https://ieeexplore.ieee.org/document/7880045>.
- [25] Mahdy, L.N., Ezzat, K.A. & Tan, Q., 2018. Smart ECG Holter Monitoring System Using Smartphone. *ResearchGate*. Available at: (https://www.researchgate.net/publication/330254182_Smart_ECG_Holter_Monitoring_System_Using_Smartphone.)
- [26] Grond, M. et al., 2013. Improved Detection of Silent Atrial Fibrillation Using 72-Hour Holter ECG in Patients With Ischemic Stroke. *PubMed*. Available at: <https://pubmed.ncbi.nlm.nih.gov/24130137/>.
- [27] Jebin, S.R. & Mohamedbeemubeen, N., 2019. Real Time Physiological Status Monitoring through Telemetry System for On-Spot-Accident Patients using IoT. *International Journal of Trend in Scientific Research and Development*. Available at: <https://www.ijtsrd.com/engineering/bio-mechanicaland-biomedical-engineering/23470/real-time-physiological-status-monitoring-through-telemetry-system-for-onspotaccident-patients-using-iot/s-rabia-jebin>.
- [28] Recording Blogs. Available at: <https://www.recordingblogs.com/wiki/low-pass-filter>.
- [29] Brainly. Available at: <https://brainly.com/question/16899401>.
- [30] Haghofer, A. et al., 2020. Evolutionary optimization of image processing for cell detection in microscopy images. Available at: <https://www.sciencedirect.com/science/article/abs/pii/S0925231220313295>.
- [31] Okili77, 2019. *Adobe Stock*. Available at: <https://stock.adobe.com/es/images/heart-anatomy-cross-section-outline-vector/134244338>.
- [32] Studica. Available at: <https://www.studica.com/national-instruments/ni-mydaq-hardware-student>.
- [33] Plux. Available at: <https://www.pluxbiosignals.com/pages/biosignalsplux>.
- [34] Amazon. Available at: <https://www.amazon.com/Rigol-DS1054Z-Digital-Oscilloscopes-Bandwidth/dp/B012938E76>.

APPENDIX 1. MatLab code for my-DAQ

This appendix provides the MatLab code that we used for my-DAQ.



```
myDAQ.m x +
1  clc; clear; close all;
2
3  %Create a DAQ session for NI hardware
4  daqlist("ni")
5  d=daq("ni")
6
7  %Add an analog input channel
8  addinput(d,"myDAQ1","ai0","Voltage")
9  d.Channels
10
11 %Read data for 5 seconds and make a table for the signal
12 tabledata=read(d);
13 matrixdata=read(d,"OutputFormat","Matrix");
14 data=read(d,seconds(5));
15 filteredECG = filterECG(seconds(data.Time), data.Variables);
16 plot(data.Time, data.Variables);
17 ylabel("Voltage(V)");
18
19 %Save the data to a CVS file
20 x=[seconds(data.Time) data.myDAQ1_ai0];
21 writematrix(x, "x.csv", 'WriteMode','append');
```

Figure AP1 1 MATLAB code for my-DAQ

APPENDIX 2. Signals from the 30 minutes experiment

This appendix provides detailed data and analysis of signals referenced in 4.2.1.

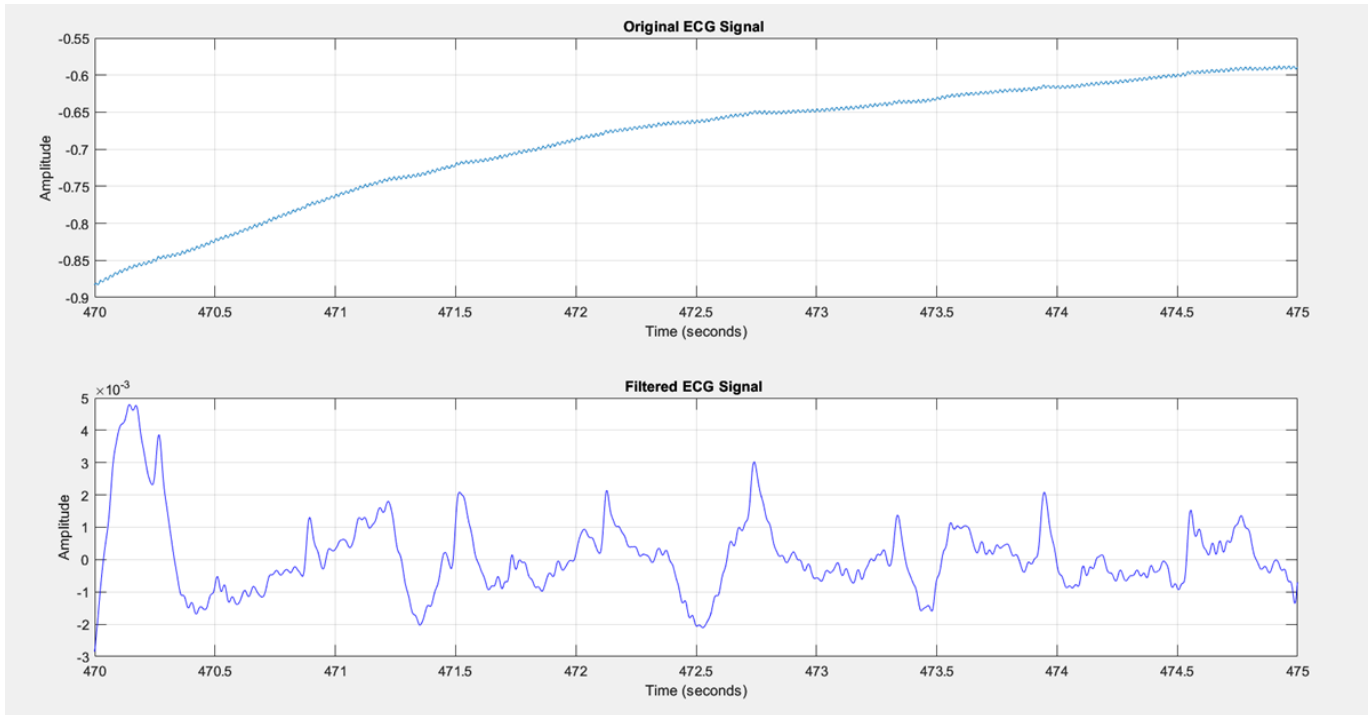


Figure AP2 1 7th minute of the 30th minutes experiment (mV/s)

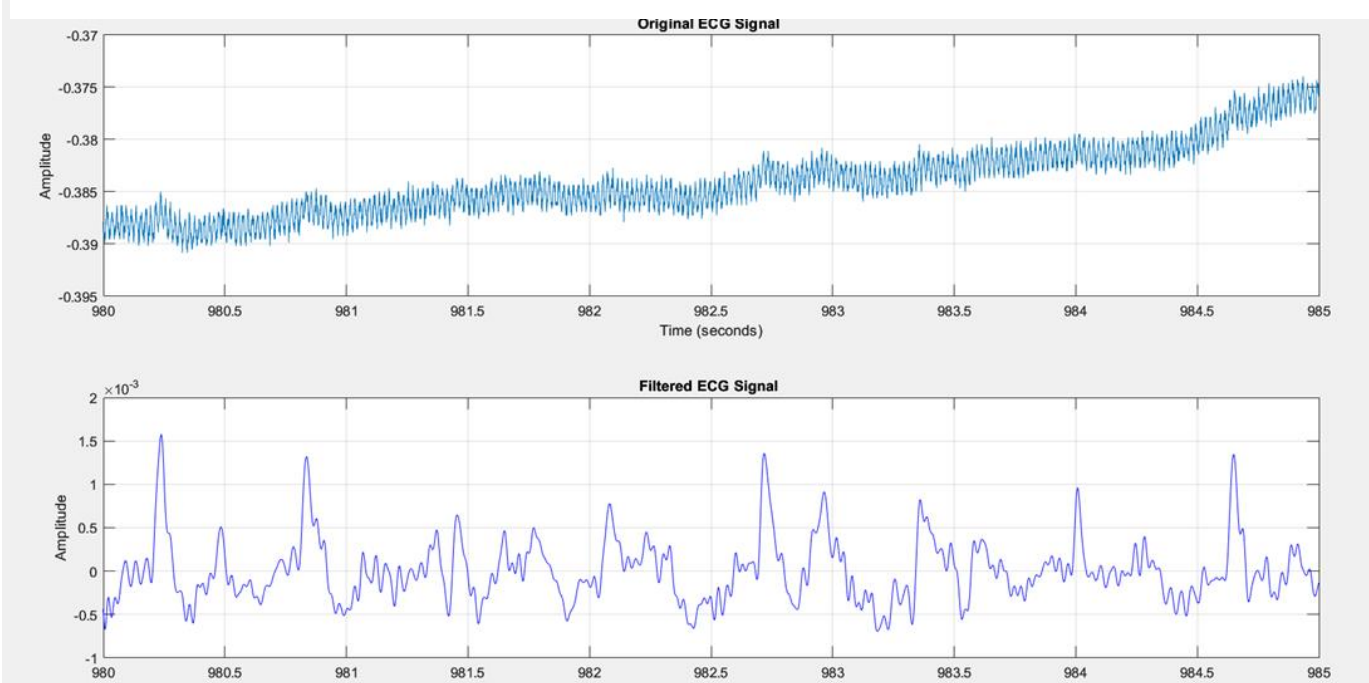


Figure AP2 2 16th minute of the 30th minutes experiment (mV/s)